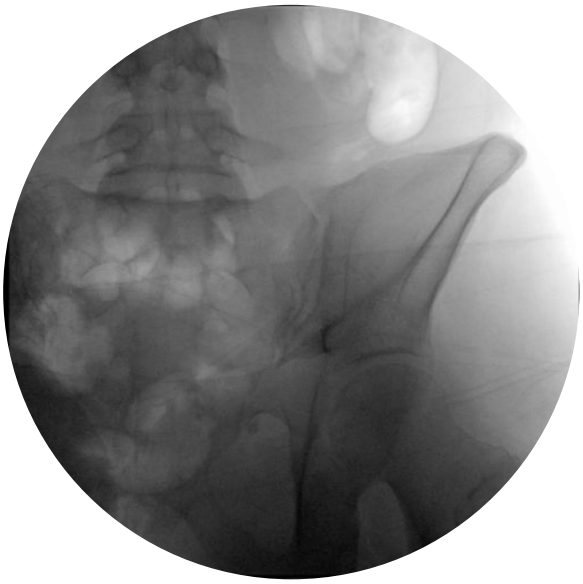

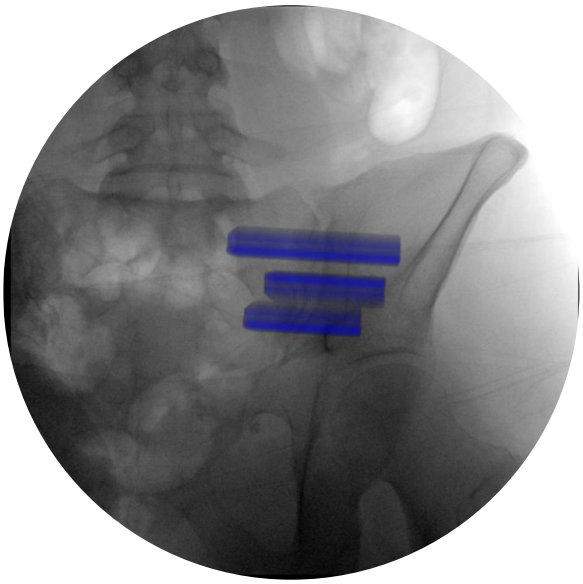

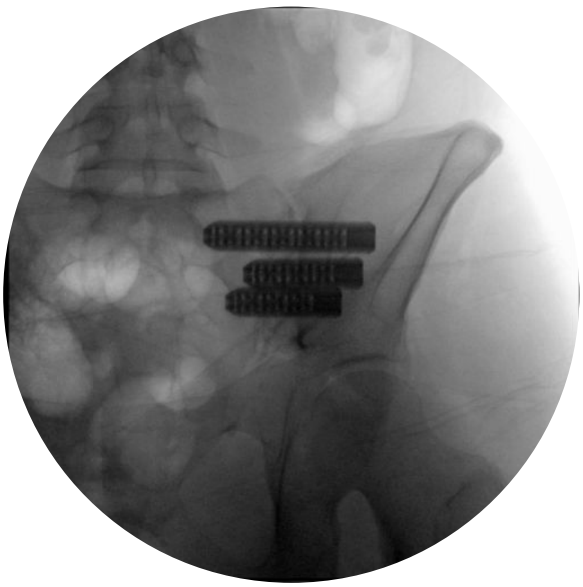

How to Improve Sacroiliac Joint Fusion Surgery?

An automated workflow with an intraoperative visualisation of the surgical planning

S. Lankheet
Master thesis Technical Medicine
July, 2023

UNIVERSITY OF TWENTE.

MST

HOW TO IMPROVE SACROILIAC JOINT FUSION SURGERY?

An automated workflow with an intraoperative visualisation of the surgical planning

---

General information

Steven Lankheet
Technical Medicine at University of Twente
Department of Orthopedic surgery and 3D medical lab MST

Graduation committee

Chairman	Prof. Dr. I. Sechopoulos
Technical supervisor	Dr. F. F. Schröder
Medical supervisor	drs. J.M. Nellensteijn
Process supervisor	E.M. Walter, MSc
External member	B. Wermelink, MSc

Colloquium

Date	18 July 2023
Time	14:00 Hour
Place	TL1133, Technohal, Hallenweg 5, 7522 NH Enschede

Preface

My academic experience started in 2015 with the bachelor Biomedical Engineering. Throughout this study I enjoyed the medical subjects and learning about the healthcare system. However, I found myself yearning for a more direct connection to clinical practice and helping patients. Therefore, I made a deliberate choice to change to Technical Medicine. Before embarking on this master's program, I had to complete 1.5 years of pre-master. Not knowing many other students, I navigated the challenges on my own. I enjoyed the technical emersion and the programming skills that were needed. I was especially intrigued by the courses on deep learning. However, when the time came for my first M2 internship, I chose a project focused on 3D printing due to my existing interest and some experience in 3D design. Fortunately, a few weeks later, I was granted my preferred choice - an internship centred around 3D printing a guide for Sacroiliac dysfunction. I didn't know what Sacroiliac dysfunction was but I liked 3D printing. However, in the first week it became apparent that the assignment did not involve 3D printing but something way more interesting: software development.

Before I dive into the story of the first internship, and also this master thesis, there were three more internships that year. Two at different cardiology departments and one at the ENT department. While these internships had either a verry interesting technical question or a direct link to the clinic there was no internship that had a combination of these two just like my first internship. Here there was a clear question from the clinic that could possibly solved with software.

In 2021 I started with this internship. Dr. Jorm Nellensteijn, my medical supervisor, was driven by a research mindset to improve the surgery he had specialised in over the last couple of years. Assisting Dr. Nellensteijn was Nick Kampkuiper, a fellow Technical Medicine student, who served as my daily supervisor. Their shared enthusiasm for Sacroiliac dysfunction got me as motivated. As revealed before, due to the motivation and the combination of technical & clinical aspects, I was verry excided that I could also do my master thesis on this subject. I want to thank Dr. Jorm Nellensteijn and Nick kampkuiper for their supervision and enthusiasm during these assignments. I want to thank Edsko Hekman en Prof. Ioannis Sechopoulos who helped to keep my work on track and I want to thank everybody at the 3D medical lab that has helped me over the last year especially Maaike Koenrades en Femke Schröder. My personal and professional development has been an important part of the internships and my thanks go's to Elyse Walter for her guidance.

I enjoyed my year at MST and learned to work hard to achieve a goal and how to integrate the clinic and technical part of the Technical Medicine master. I eagerly anticipate what the future holds.

Contents

List of abbreviations

AP	Anterior-posterior
CT	Computed tomography
CAS	Computer-assisted surgery
CF	Conventional fluoroscopic
CB	Cortical breach
CE	Cortical encroachment
DRR	Digitally reconstructed radiograph
HDD	Hausdorff distance
MDR	Medical device regulation
MIS	Minimally invasive surgery
PA	Posterior-anterior
SI	Sacroiliac
SIJF	Sacroiliac joint fusion
SD	Standard deviation
VSP	Virtual surgical planning

0 General Introduction

The sacroiliac (SI) joint is the largest axial joint and connects the lumbar spine with the pelvis [1]. SI dysfunction may cause low back pain and debilitation, yet dysfunction of the SI joint is often missed as a cause for low back pain [2]. The underdiagnosis of SI dysfunction is sustained by the complexity of diagnosis [3]. The diagnosis relies on a combination of patient history, clinical examination, and diagnostic injections [2, 4]. The most described physical examinations are "distraction", "thigh thrust", "compression", "FABER", and "Gaenslen" [2, 3, 5]. While these tests individually have limited reliability, a positive result in at least three tests is a reliable indication for SI dysfunction [3]. In addition, a diagnostic SI joint injection with a local anaesthetic is performed to confirm the diagnosis further. Physical therapy and therapeutic SI joint injections can improve patient outcomes [6]. If these therapies no longer suffice, surgical fusing of the affected SI joint can be an option. This can be achieved through a posterior or lateral approach to insert implants or a graft [7]. Minimally invasive SI joint fusion (SIJF) using three triangular implants placed using the lateral approach, see fig. 1, has proven to be safe and to have good outcomes [2, 8, 9].

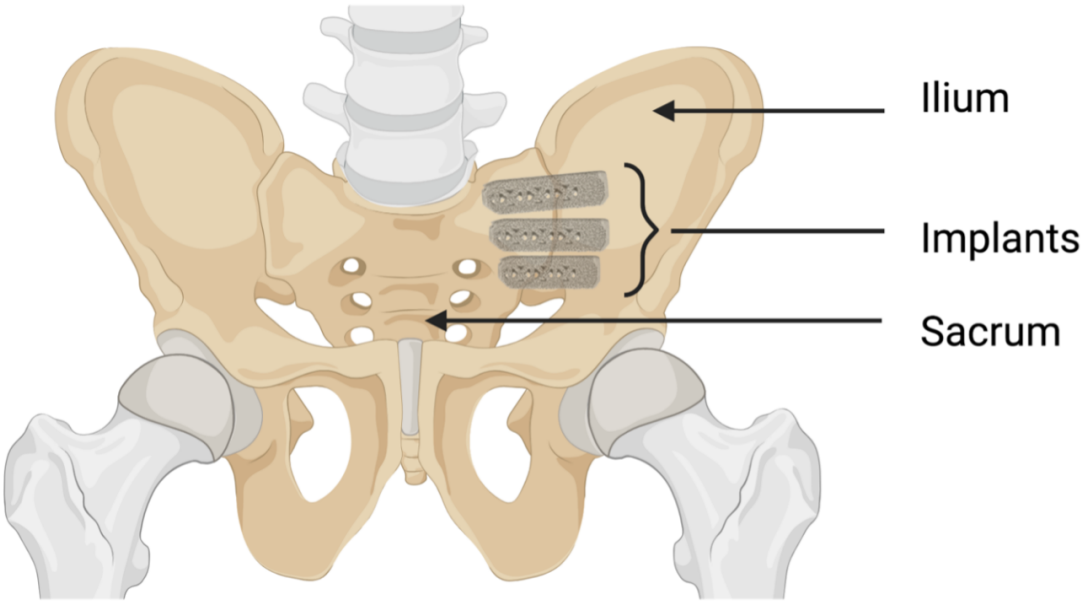

Figure 1: Anterior posterior view of the pelvis with three iFuse implants through the left SI joint.

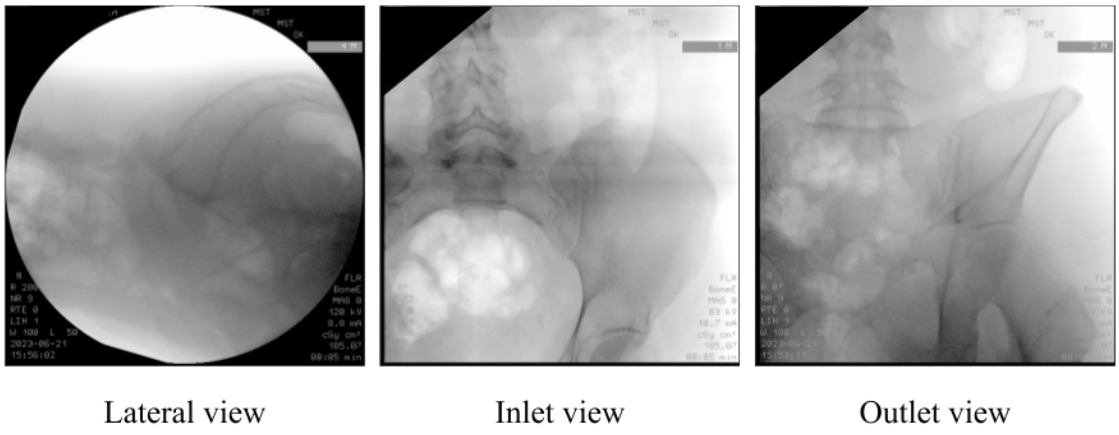

Figure 2: The fluoroscopic views used during sacroiliac fusion surgery.

During SI joint fusion surgery, conventional fluoroscopic (CF) guidance is used when placing the implants. A guide wire is used to position the implants. CF guidance allows lateral, inlet, and outlet views (see fig. 2) to monitor the guide wire placement. During insertion, important structures like the L5 nerve and the S1 and S2 foramen must be avoided. Incorrect placement can lead to severe complications such as neurovascular damage. Within the sacrum, there is some flexibility in safe placement of the implants [10]. Some studies have described possible optimal configurations that result in better stability, such as placing the implants in a triangular configuration [10–12]. Better stability could result in less implant loosening and better patient outcome. To reduce the complication rate, and to place the implants in an optimal configuration, a virtual surgical planning (VSP)(see fig. 3) can be constructed.

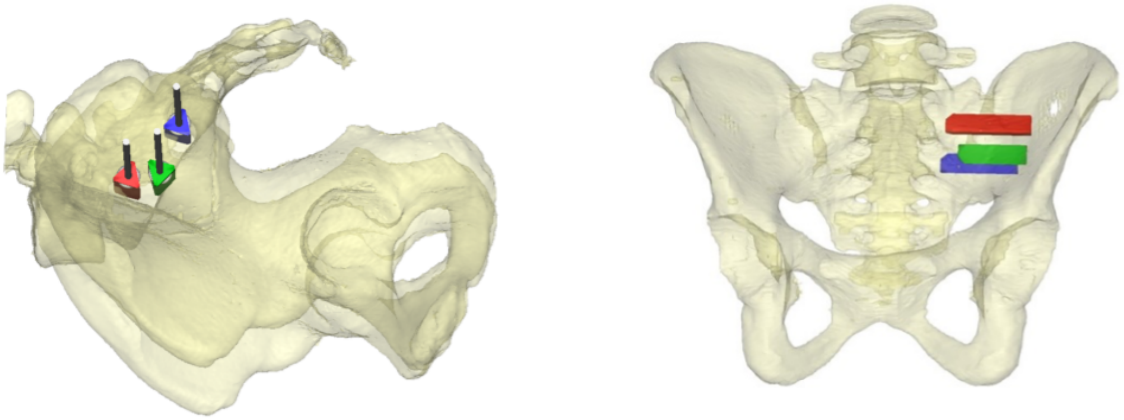

(a) Lateral view

(b) Anterior-Posterior view

Figure 3: Virtual surgical planning (VSP), the CT-based VSP of the three triangular planned implants (red, green, and blue) is depicted with bone displayed slightly transparent. In the lateral image (a), the guide pins are shown.

This preoperative planning consists of the optimal patient-specific implant configuration, based on a computed tomography (CT) scan, while including a safety margin. It can be challenging to recreate the VSP accurately during surgery. Additional techniques can aid in guiding the recreation of the VSP. For example, computer-assisted tracking of the patients' pelvis and of surgical instruments could be used to guide free-handed insertion by providing real time feedback. Secondly, the use of robotic arms that determine the drill position and guide wire placement. The use of tracking devices and robotic arms can

increase placement accuracy and decrease surgical time. However, they are far more expensive than CF guidance and not available in most hospitals. Therefore, SI implant placement is performed free-handed using CF guidance in the Netherlands. With the use of CF, the process of percutaneous guide wire placement has been described as "trial and error" [13]. This is due to the limitation of visualising one view at a time. In addition, the divergence of the radiation beam results in fluoroscopic parallax, making it difficult to compare the VSP with the fluoroscopic image. Most importantly, using a suboptimal lateral view, in which the patient is not orientated properly, could result in incorrect placement. In such cases, the location of the implants can deviate from the planned position and could surpass the safety margins.

One method of improving the useability of CF is to use Digitally Reconstructed Radiographs (DRRs). These virtual fluoroscopic images can be created from CT data including anatomical structures. Superimposing DRRs onto the CF images during surgery, creates additional guidance by highlighting anatomical structures of interest. Previous research has shown the implementation of superimposing the foramen during SIJF [14]. With this method, it is also possible to create DRRs of the guide wires as planned in the VSP and superimpose the position of the guide wires onto intraoperative CF images. Superimposing involves the overlay of important elements of an image onto a base image.

To integrate the workflow into routine clinical care, it must be developed in accordance with the Medical Device Regulation (MDR) guidelines [15]. Clinical implementation is expected to reduce the trial-and-error process and thereby reducing surgery time and increasing the accuracy which the VSP is reproduced. Implementing this method requires programming of new features in dedicated medical software, developing a protocol, doing risk analysis and extensive testing.

The aim of this thesis is, therefore, improve perioperative CF guidance by superimposing DRR onto the CF images during SIJF for patients with SI dysfunction. This goal is reached by first, determining the effects of C-arm placement (Chapter 1). Second, developing software to superimpose the VSP onto perioperative CF images (Chapter 2). Third, developing a workflow within MDR guidelines to clinically implement the software during SIJF (Chapter 3). Last, clinical testing of the developed software and workflow and comparison to standard SIJF surgery (Chapter 4).

1

The Clinical Use and Impact of C-arm Placement for Obtaining a True Lateral Pelvic View

Abstract

Introduction - Minimally invasive sacroiliac joint fixation is performed with conventional fluoroscopy to visualise the anatomy and guide percutaneous insertion of guide-wires. Incorrect use of fluoroscopic guidance and subsequent incorrect placement of the guide-wires can damage nearby neurovascular structures. This study aims to assess the knowledge gap among surgeons regarding the appropriate utilization of fluoroscopic guidance, specifically the C-arm and its correct positioning. Furthermore, the clinical implications of misalignment in C-arm placement will be explored.

Method - A 11-item questionnaire focusing on the operational principles of a C-arm and on obtaining lateral views was sent to surgeons from ten orthopaedic and trauma departments. The participating surgeons were categorised into two groups based on their level of experience. To assess the clinical impact of C-arm misplacement, phantom experiments were conducted. Five 3D printed pelvises were positioned in a lateral alignment with the C-arm. Subsequently, the C-arm was translated, mimicking a suboptimal position, and the pelvis's were rotated to compensate for the translation. A virtual surgical planning, containing iFuse implants and SI screws, was created for each pelvis and was adjusted for the determined rotation at the translated C-arm position. The positioning of the new implant and screw positioning was checked for instances of breaching.

Results - Eight surgeons responded, half of whom were classified as experienced. There was no significant difference in the knowledge questions between the two groups. Only 75% of the surgeons noted the importance of superimposing the iliac cortical densities to obtain a true lateral image. In the phantom experiments, an average of 4.2 ± 0.95 degrees compensating rotation was needed for a 5 cm translation of the C-arm. Of the 45 virtually placed iFuse implants at the rotated position 7% showed cortical breach. For the 30 virtually placed SI screws 63% showed cortical breach.

Conclusion - Surgeons in both the experienced and in experienced group have exhibited a knowledge gap on the operational principals of the C-arm. In addition, there was no consensus on optimal C-arm placement among the respondents. The experimental findings clearly demonstrate that misplacing the C-arm is associated with rotational disparities, which, in clinical practice may result in a suboptimal implant position with an increased risk for complications.

1.1 Introduction

A substantial part of orthopaedic surgery is dedicated to the pelvic area. Pelvic fractures make up around 10% of patients admitted with blunt trauma [16]. Pelvic fractures have been treated with open reduction and stabilisation ,however, they have a high rate of complications [17]. A shift to minimally invasive surgery (MIS) has reduced wound complications and infection rates [17]. In addition to pelvic fractures, sacroiliac (SI) joint dysfunction can cause debilitating pain and can require surgical intervention. Open SI joint fixation (SIJF) was described first as a treatment for SI joint dysfunction. Recently, MIS techniques have shown improved patient outcomes [18]. In both surgeries, MIS techniques often consist of a percutaneous screw or implant placement. During surgery, conventional fluoroscopic (CF) guidance can be used to visualise bony anatomy and guide the percutaneous insertion of guide-wires. However, with CF guidance safe placement can be challenging, due to the complex 3D bone morphology of the sacrum and closely located neurovascular structures [19]. Incorrect placement can lead to perforating the neural foramina and cause irreversible damage.

The use of CF guidance during MIS during pelvic surgery has some disadvantages. First, a major disadvantage of CF imaging is the limited visibility of the pelvic bone [20]. This is especially the case in a lateral view, where the increased body thickness results in lower image contrast. Second, obesity and bowel gas can further reduce the visibility of important anatomical structures such as the neural foramina. Third, a limitation of CF guidance is the need to verify every motion of the insertion of the guide-wire in the lateral, inlet, and outlet view [21]. Using standardised angles (e.g., 30°and 45°) for each patient does not provide optimal visualisation and could result in incorrect views [22]. Using incorrect views increases the risk of overlooked errors [23]. Therefore, free-handed placement of screws and implants requires a high degree of fluoroscopic image knowledge and 3D thinking.

Previous research has described the use of CF guidance during percutaneous screw placement as “trial and error” [13], resulting in challenging implant placement with complications as high as 21% [24]. Several methods were developed to reduce “trial and error” and the complication rate. Computer-assisted surgery (CAS) uses tracking of the C-arm, pelvis, and surgical tools to provide additional guidance. Research by Verbeek et al., found no reduction in complication rate with CAS [20]. They did find that experienced surgeons had lower complication rates for both the CAS and CF placed screws. Less experienced surgeons may lack sufficient knowledge of the working principles of CF and the X-ray beam. When using CF, it is crucial to consider the working principles, such as the divergence of the X-ray beam and parallax distortion. The divergence of the X-ray beam results in relatively different anatomical magnifications and parallax distortion. By translating the centre of the C-arm, parallax distortion can dramatically change relative distances between anatomical structures. Incorrect placement of the C-arm may increase the complication rate. While literature has discussed obtaining optimal views taking the working principles into account [22], the clinical relevance of the placement of the centre of the fluoroscopic beam has not been addressed.

We expect that not all surgeons fully know how to use the C-arm optimally. To obtain this insight and improve potential knowledge gaps, the aim of this study is twofold. First, the potential knowledge gaps related to C-arm placement during CF-guided pelvic surgery are assessed using a questionnaire. Second, the theoretical principles of C-arm placement are demonstrated to help surgeons understand the clinical impact of incorrect use of the C-arm. We expect that understanding of CF guidance will provide a foundation for obtaining optimal visualisation during pelvic surgery. This may reduce the complications associated with misplaced SI implants and screws.

1.2 Materials and methods

1.2.1 Survey

A 11-item questionnaire was developed in Microsoft Office 365 Forms (Microsoft, Redmond, USA) to assess surgeons' experiences at pelvic trauma centres using C-arm fluoroscopy (Appendix A). The questionnaire contains three parts: (i) determining the experience with surgical treatment of pelvic fractures and assessing their competence; (ii) testing their knowledge on the magnification principle of a C-arm; and (iii) testing their knowledge on obtaining lateral views during pelvic surgery.

In May 2021, the web-based questionnaire was distributed to surgeons from ten hospitals using an invitation e-mail. These are surgeons from orthopaedic and trauma departments specialised in pelvic surgery located in the Netherlands. A reminder e-mail was sent out to surgeons who had not initially responded, and the questionnaire was closed in June 2023.

The survey data was analysed using SPSS version 28 (SPSS Inc., Chicago, USA). Questions 3–11 were stratified by experience of the surgeon. If differences between the two groups was found, statistical analysis was performed to determine the significance. For the self-scored experience, multiple unaired t tests were performed. For the categorical answers, a two-sided chi-square test was performed.

1.2.2 C-arm placement experiment

To illustrate the effect of incorrect use of the C-arm and to obtain a true lateral view in clinical practice, some phantom experiments are performed. Realistic phantoms featuring varied anatomies were created using pelvic CT scans that were segmented and 3D printed. The experiment consists of obtaining fluoroscopic C-arm images at different angles and positions.

Retrospectively, a pelvic CT-scan was obtained from five patients who had been surgically treated for SI dysfunction from 2021 to july 2022 in Medical Spectrum Twente hospital (Enschede, Netherlands). For the inclusion a minimal resolution of the CT scan was slice thickness, 0.9 mm; pixel spacing, 0.79 by 0.79 mm was required. No CT-scans were excluded based on anatomy variances. Ethical approval for retrospective and prospective analysis of VSP was obtained in July 2022 from the Research Ethic Committee of MST (nWMO study, K22-24). The requirement for written informed consent was hereby waived for this retrospective analysis.

Using Materialise Mimics 25.0 (Materialise, Leuven, Belgium), a (semi-)automatic segmentation of the L5, sacrum, ilium, and proximal femurs was created. The segmentations were combined in a single model with fixture points at the cranial and caudal side. The models were exported to an opensource 3D slicer to create the G-code files and printed with white polylactic acid on a scale of 1:1 with 3-layer wall thickness and 15% infill on a Ultimaker 3D printer (Ultimaking Ltd. Geldermalsen, Netherlands).

The 3D printed models were fixed in a rotation device which allows computer-controlled rotation along the vertical and sagittal axis in steps of 0.5 degrees. Next, the C-arm was positioned to acquire a lateral fluoroscopic image of the pelvis using a Ziehm Vision FD C-arm (Ziehm Imaging GmbH, Nuremberg, Germany), see fig. 1.1. Here the central ray is positioned at the centre of the sacral alae. Next, the pelvis is rotated along the vertical and sagittal axis to superimpose the iliac cortical densities. Here the distance between the iliac notches should equal the distance between the pelvic crests. This view is defined as true lateral.

Next the C-arm is translated to (A) 5cm posterior, (B) 5cm posterior and 5cm caudal, and (C) 5cm caudal, see fig. 1.2. The iliac cortical densities are superimposed at each location using the computer-controlled rotation device by rotating the pelvis. Here the angle of rotation needed to superimpose the iliac cortical densities is denoted with the true lateral as a reference.

Figure 1.1: Experimental setup with (A) the C-arm monitor and laptop with rotation control software and (B) the C-arm with rotation device and 3D printed pelvis.

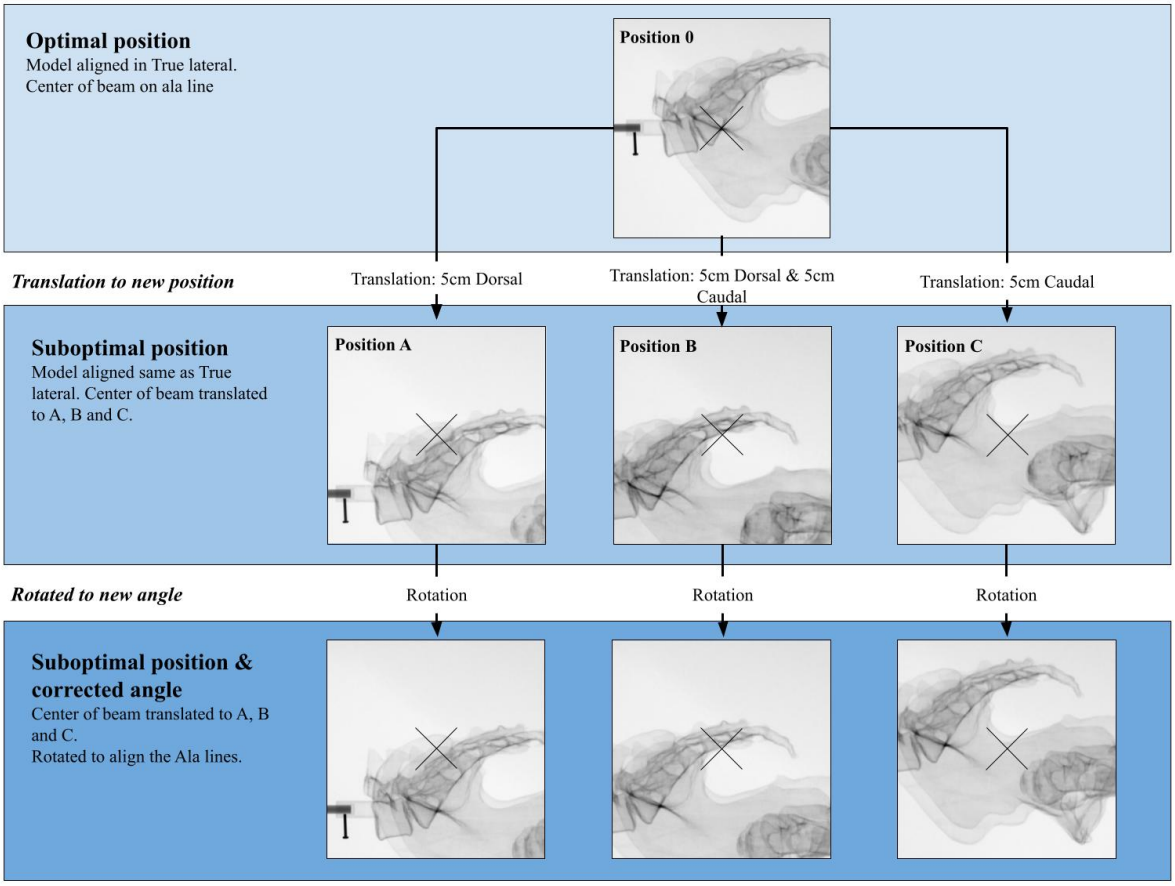

Figure 1.2: Workflow for obtaining the rotation angle needed to align the ala lines at three positions (A, B and C) with the true lateral as reference.

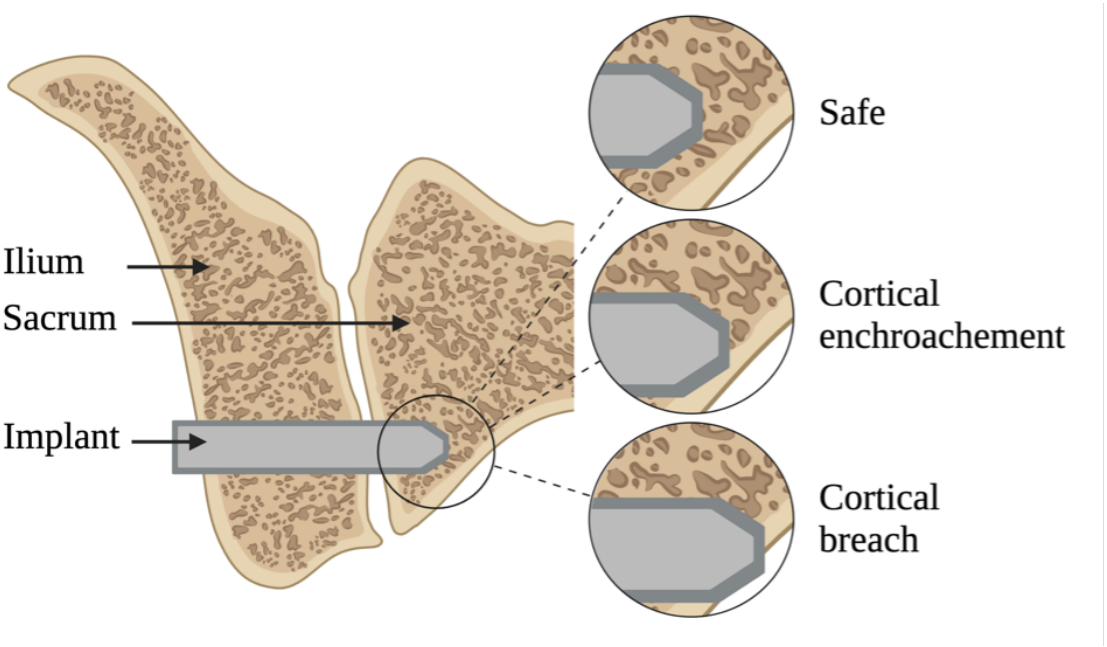

Figure 1.3: Schematic depiction of a coronal cross-section of the SI joint with a implant in situ. Three possible outcomes for the placed implants.

Based on each CT scan, two patient-specific virtual surgical plannings (VSP's) are constructed using Materialise Mimics 25.0 (Materialise, Leuven, Belgium). The first VSP consists of three triangular SI implants and the second consist of two SI screws. Next, each VSP is duplicated and rotated for the angles obtained at position A, B, and C (as described in fig. 1.2). For each position the VSP is checked on the safety margin, implants are scored as "safe", cortical encroachment (CE), and "cortical breach" (CB), see fig 1.3. CE and CB are considered minor and major complications during spine surgery[25].

1.3 Results

1.3.1 Survey

From the total of 8 surgeons who responded, 4 were classified as experienced with the placement of SI screws. All surgeons in this group reported to have more than 10 years of experience. Of the 4 surgeons classified as inexperienced, all 4 reported having 5 or fewer years of experience. In both groups, 2 surgeons reported performing 5 to 20 operations, and 2 surgeons reported to perform 1 to 5 operations every year. A complete overview of the results is shown in fig. 1.4. There were no significant differences between the experienced and inexperienced respondents in any questions. However, the in experienced surgeons performed worse on scoring important factors to obtain a lateral view (Q5), the effect of moving the patient closer to source (Q6) and how each side of the patient is visualised (Q7). One surgeon in each group chose a position of the central ray outside the S1. Most surgeons, 79%, successfully determined if the images given were true lateral (Q9-Q11).

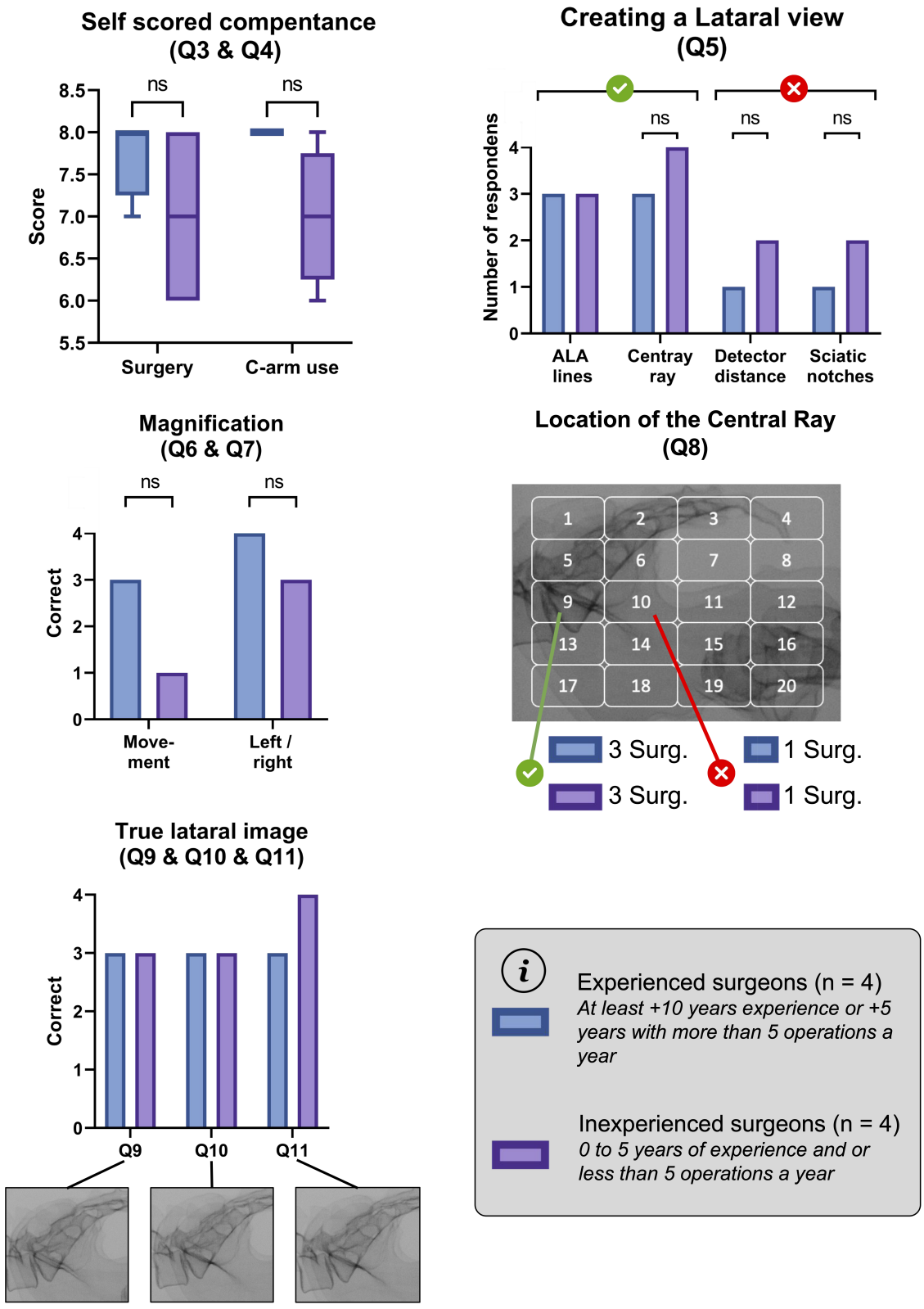

Figure 1.4: Overview of the survey results among surgeons on their experience and knowledge on the placement of SI-screws.

1.3.2 C-arm placement experiment

Each of the five pelvis models was successfully positioned in a lateral alignment within the C-arm, creating the true lateral image before translating to a new position (see fig. 1.5). The average rotation at each position was 3.9 ± 0.7° along the longitudinal axis (Long-ax) and 0.2 ± 0.4° sagittal axis (Sag-ax) (Position A), 3.5±0.5° Long-ax and 4.6±1.3° Sag-ax (Position B), and -0.1 ± 0.2° Long-ax and 4.6 ± 1.0° Sag-ax (Position C). The implants were virtually placed using the obtained angles for each position. Of the 45 virtually placed iFuse implants, 14 (31%) showed cortical encroachment and 3 (7%) showed cortical breach. Of the 30 virtually placed SI screws, 9 (30%) showed cortical encroachment and 19 (63%) showed Cortical breach.

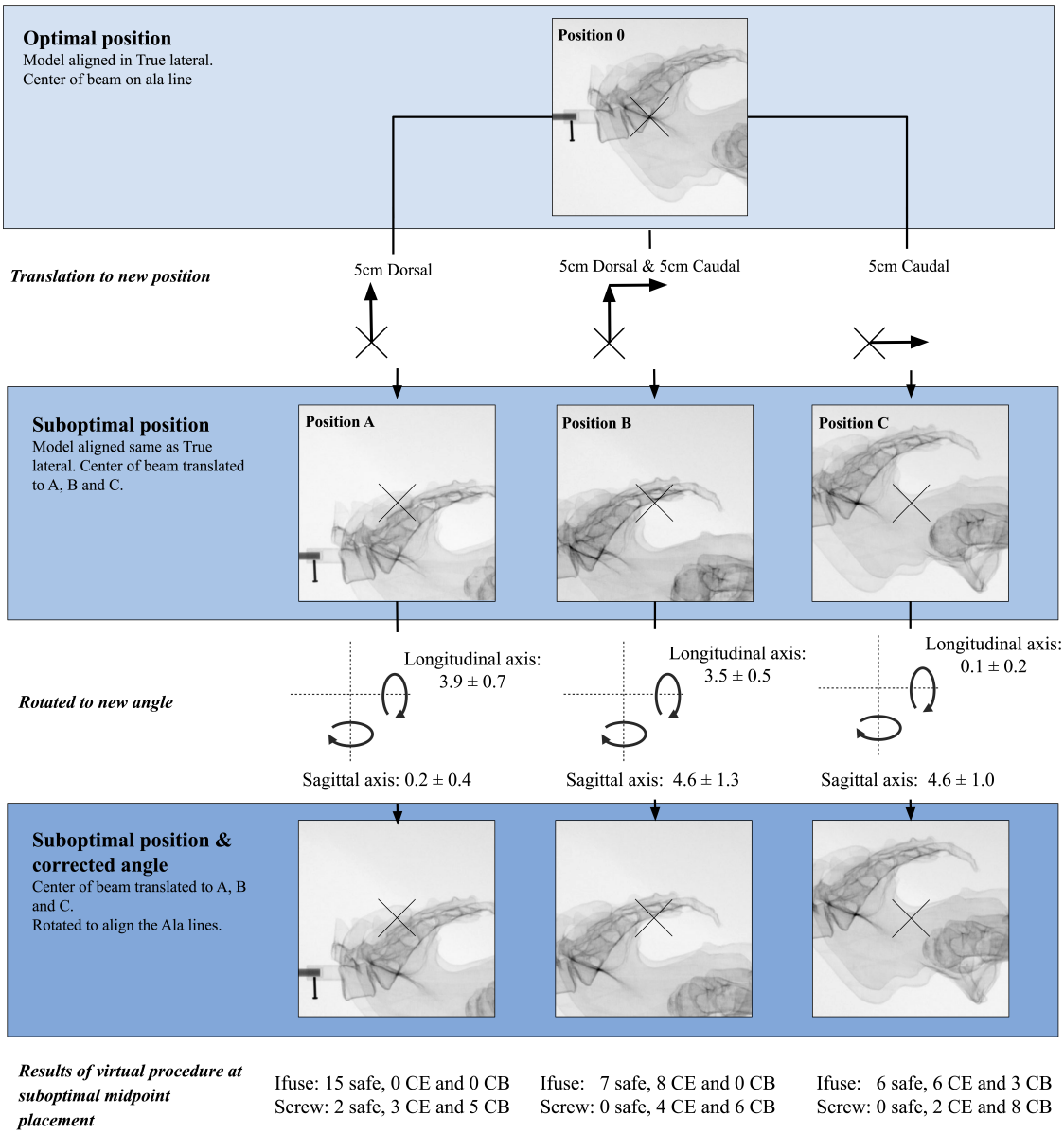

Figure 1.5: Overview of the three positions obtained relatively from true lateral. At each location, the image with the superimposed ala lines is shown with the average rotation needed to obtain these images. The iFuse and SI screws at each location are reviewed for safe implant positions, cortical encroachment (CE) and cortical breach (CB).

1.4 Discussion

In this study, first, the knowledge gaps related to C-arm placement during CF-guided pelvic surgery were assessed. The survey data suggest that surgeons have limited knowledge regarding the optimal placement of the C-arm to obtain true lateral views during CF-guided pelvic surgery. Second, the theoretical principles of C-arm placement and its clinical impact were demonstrated. Results showed small C-arm translations can be compensated by rotating the patient, resulting in difficult to distinguishable images. If implants are placed without compensating for this new rotation, 7% of the iFuse implants and 63% of the SI screws would show severe complications in a clinical setting.

The lateral view is seen as the most important view during SI Screw placement [26, 27]. To obtain this view, literature describes the importance of superimposing the iliac cortical densities [27, 28]. Our survey data indicated that 75% of the surgeons are aware of this. On the other hand, existing literature presents conflicting opinions regarding the position of central ray for obtaining true lateral views. Some sources do mention the need to centre the view on the S1 however, they suggest a true lateral is obtained when the sciatic notches are overlapping [27, 28]. In contrast, one study centred the image on the superimposed sciatic notches[29]. Superimposing the sciatic notches is also mentioned in literature where the position of the C-arm is not discussed [22, 30]. 3 of the 8 surgeons did choose superimposing the sciatic notches as important. In addition to the conflicting information on obtaining true lateral views, some articles show "true lateral" views that are not centred at the S1[6, 31, 32]. The survey data showed that 79% of the surgeons were successful in determining if a lateral view is true lateral. The use of incorrect views during surgery increases the risk of complications [23], which remains a limitation of CF guidance. CAS has emerged as a potential solution to overcome this limitation of CF. Previous studies have shown that CAS may lead to a reduction in complications [24, 33, 34]. Despite these findings, some have reported no significant benefits [20]. Nonetheless, a global survey of spine surgeons indicated that 87% of them use CF in daily use, while only 11% use CAS [35], highlighting the importance of understanding how to obtain accurate views using CF.

The survey includes multiple surgeons from several level 1 trauma centres, providing a understanding of the knowledge of both experienced and inexperienced surgeons. As a result, the impact of hospital-specific training for surgeons or radiology assistants is minimised. Secondly, the study's utilisation of phantoms and a computer-controlled rotation device permits precise measurements. Angular adjustments of half a degree as used in this experiment, are not feasible with a conventional patient and C-arm setup. Thirdly, the study's testing of various anatomies and evaluation of the impact on both SI screws and implants broadens its clinical relevance. Although the use of CF for the insertion of both screws and implants shares similarities, they are often discussed separately. The essential factors for obtaining a lateral view are applicable for both screws and implants.

The survey conducted in this study has limitations. Firstly, the use of a closed-ended survey with pre-designed answer options may lead to suggestive questions, thereby limiting the true representation of the use of CF by the surgeon. To mitigate this concern to the best extent possible, the survey underwent thorough testing and extensive review by multiple surgeons and residents. Their input aimed to ensure the survey's appropriateness and minimize the impact of suggestive questioning. Secondly, the low number of surgeons who participated in the survey is a limitation that may limit the generalizability of the study findings. Lastly, categorizing the surgeons as experienced and inexperienced based on years of experience alone may be inadequate. For instance, a surgeon who has conducted 15 surgeries in two years may be more adequate than a surgeon with 20 surgeries over a span of 10 years. Therefore, this approach may fail to capture nuances in the surgeon's experience.

Some limitations to the experiment may restrict its applicability to clinical settings. Firstly, the direct consequence of complications resulting from rotation does not entirely represent actual surgery. Surgery involves checking the direction and safety margins in multiple views. Furthermore, guide wires are typically used prior to implant or screw placement, to allow for adjusting the position if necessary. Nonetheless, it has demonstrated that even minor rotations in positioning can result in complications, underscoring the significance of using the correct views. Secondly, virtually placed implants' safety depends

largely on the patient's anatomy. Due to large anatomical differences between patients, generalisation of these results to the clinic is limited. To ensure equitable complication rates, the virtual planning is constructed with the largest safety margin in all directions. Lastly, a single individual reviewed the true lateral view and subsequent lateral views. This can result in bias and other observers may select different angles.

The study's findings have important clinical relevance for surgeons performing minimally invasive SI joint reduction using SI screws and SI joint fixation using iFuse implants, where CF is used to guide the insertion of guide-wires. Findings from the questionnaire indicate that there exists a knowledge gap among pelvic surgeons regarding the use of CF in pelvic surgery. Especially in obtaining the true lateral view. Findings from the experiment have highlighted potential adverse events resulting from incorrect use of CF. These finding combined emphasised the need for increased clinical insight. This can be achieved by incorporating awareness of CF use in training and refresher courses for surgeons, ultimately leading to improved patient outcomes and reduced complication rates.

1.5 Conclusion

Sacroiliac joint fixation using screws or implants remains challenging due to anatomical variations and to the closely located vulnerable neurovascular structures. CF guidance is used during sacroiliac joint fixation, which makes a comprehensive understanding of the C-arm crucial. Regarding the C-arm's operational principles, the survey revealed knowledge gaps among experienced and inexperienced surgeons. Furthermore, there was no consensus among the respondents on optimal C-arm placement during sacroiliac joint fixation. The evaluation of different C-arm positions in the phantom experiment demonstrated rotational disparities to compensate for different C-arm positions. Which in clinical practice may result in a suboptimal implant position with an increased risk for complications. Improving surgeons' knowledge gaps could enhance the safety and success of sacroiliac joint fixation surgery.

3

Automation of the SI fusion Virtual Surgical Planning Pipeline; from CT scan to Perioperative Visualisation

Abstract

Introduction - Virtual surgical planning for sacroiliac joint fusion, in which implants are planned in a patient specific position, has become standard clinical care in our hospital. The current method is time consuming. In addition, the method for intraoperative visualisation of the planning as mentioned in Chapter 2 is prone to observer error. The present study aimed to develop and preclinically evaluate an automated workflow for the fast and reliable creation and intraoperative visualisation of virtual surgical planning for sacroiliac joint fixation surgery.

Method - The workflow for creating and visualising of the virtual surgical planning was developed using the scripting module of the CE-marked Materialise software. To intraoperatively register the planning onto fluoroscopic images, convolutional deep learning networks were trained to detect at which angle the intraoperative image was captured. Evaluation metrics included the average absolute error and the percentage of images with errors below 0.5 degrees. The developed workflow was preclinically evaluated and compared to the manual workflow.

Results - Results from the automated workflow for the creation of the planning showed a significantly reduced workload for users and provided prompt guidance for each step, enhancing protocol adherence. The automated workflow reduced the time by 44 $\pm$ 7.8 % compared to the manual workflow. No clinical differences were observed between the virtual surgical plannings created by both workflows. For the intraoperative registration of the workflow, the best-performing deep learning network detected the angles from an image with a mean accuracy of 1.36 degrees on the validation dataset. In addition, 37% of the images were scored with an error less than 0.5 degrees, meaning that 63% had an error larger that the required limit for clinical use.

Conclusion - Although the accuracy of the deep learning model for intra-operative image registration did not meet the required threshold for clinical use, the (semi)-automated workflow for creating the planning generated clinically equivalent 3D models and safe virtual surgical plannings in significantly less time. Implementation of this automation reduces dependence on individual operators and improves adherence to established protocols, making it suitable for standard clinical care.

3.1 Introduction

The integration of technical innovation in clinical settings has revolutionised patient care and improved clinical outcomes. However, the implementation of these technical innovations has not been without challenges. Specifically, the creation of virtual surgical planning (VSP) is time consuming and can be prone to observer error. Sacroiliac joint fusion surgery (SIJF) is a complex surgical procedure that requires careful preoperative planning and intraoperative visualisation. The success of this procedure depends on the accurate placement of implants and avoiding damage to vulnerable surrounding anatomical structures. To achieve this, VSP and perioperative visualisation can offer guidance. Manual construction of VSP for SIJF has been successfully implemented in our hospital and has shown a reduction in complications. However, the current workflow the creation of the VSP is time-consuming. In addition, the perioperative visualisation of VSP (as mentioned in Chapter 2) has not yet been implemented in the clinic, due to the fact that it is time-consuming and prone to observer errors. Clinical validation of the benefit of the perioperative visualisation of VSP on top of CF images, is hampered by these intrinsic problems.

To reduce the time required for the full SIJF VSP pipeline and to clinically implement the perioperative visualisation, this labour-intensive and observer-dependent process must be automated within the MDR and ISO guidelines. The first step in this pipeline involves extracting the pelvis, sacrum, and SI joint from the preoperative CT scan. Manual segmentation of these structures can be tedious due to the multiple steps required, such as a combination of thresholding, morphological, and manual operations [52]. While semi-automatic algorithms can reduce segmentation time and minimise inter-observer differences, they still require manual operations. To maximally reduce the labours tasks for skilled personnel, a fully automatic segmentation algorithm is required. Deep learning algorithms for medical image segmentation have demonstrated fast and precise segmentations [53, 54]. Once the correct segmentations are obtained, the next step in the SI fusion pipeline is to determine the implant configuration. In order to automatically obtain the implant configuration researchers in other medical fields have used automatic atlas-based workflows [55]. Creating an automatic atlas-based workflow for SIJF is challenging due to the variability in size and shape of the sacrum [56] and limited knowledge on optimal implant placement. Finally, in the SIJF VSP pipeline, perioperative visualisation is required, which involves generating digitally reconstructed radiographs (DRRs) using the same parameters as the intraoperative image. The workflow, as mentioned in Chapter 2, described a method of manually determining these parameters. Deep learning models can detect these parameters from a single intraoperative image [51, 57].

Therefore, in this chapter, we develop a new workflow that combines these existing automation solutions to create an (semi-)automatic workflow from CT scan to perioperative visualisation. The proposed solution aims to reduce the manual steps involved in SIJF VSP and perioperative visualisation, decrease planning time, and minimise observer errors. This allows for accessible implementation for routine clinical care of SIJF.

3.2 Methods

The (semi-)automatic workflow was developed using the scripting module of Materialise Mimics 23.0 (Materialise, Leuven, Belgium). This allows for the implementation of Python for the (semi-)automatic creation and perioperative visualisation of the VSP. The implementation was achieved through the execution of Python commands that communicated with the CE-marked Materialise software via the Application Programming Interface (API). First, the segmentation workflow is addressed to obtain a 3D model of the relevant structures. Second, the implant placement workflow is automated to obtain the preoperative VSP. Next, the preparation workflow of the intraoperative visualisation is addressed and finally the perioperative visualisation itself. The final part consists of automating the existing workflow and developing a deep learning based workflow. Each part of the workflow was subsequently evaluated based on the input required, its robustness, performance, and safety. To evaluate the models created with the developed workflow, VSPs are created using the developed workflow from five different CT scans by an experienced user. These CT scans included males & females, left & right sided, and sclerotic & osteoporotic bone. The steps from the manual workflow

were performed to obtain VSPs from the same CT scans. The order of model creation using the automatic and manual workflow was randomized. Additionally, an inexperienced user created the VSP from a CT scan manually and with the software. This user also scored the software on ease of use.

3.2.1 3D model creation

The workflow for segmenting the pelvis and the SI joint involved seven segmentation steps, including thresholding, region growing, and filling, as well as two workflow operations: renaming and recolouring. Each step was automated using the API. The obtained models for each of the five patients were compared on volume, surface distance and creation time.

3.2.2 Implant positioning

The virtual placement of the implants required obtaining a lateral view, loading the implants, moving them, and changing them to different sizes. Obtaining the lateral view required manual input from the user and could not be automated; however, scripting was used to guide this process and recreate the same view in multiple steps of the workflow. Currently in the manual workflow, two STL files are loaded for each implant, containing the implant and implant cylinder respectively. These loaded STL files are imported at the origin and needs to be manually moved to the desired location. Changing the size of the implant involved loading two new STL files, moving them to the position of the old implant, and removing the old STL files. To facilitate these processes, a graphical user interface was created to allow the user to load and change implants sizes. Implants are automatically aligned laterally and the distance between implants can be calculated by the script.

The time to obtain the VSP manually and automatically from the 3D models was compared for the five patients and for the inexperienced user.

3.2.3 Preoperative VSP visualization

After obtaining the VSP's, the software allows users to create 3D inlet, outlet, and lateral views, and automatically saves screenshots. These are automatically populated into a slideshow template with the patients' data. Using the fluoroscopy function of Mimics, the software creates a true lateral digital radiograph (DRR) of the anatomical 3D model. Users can then create inlet and outlet DRRs. These views are automatically created with the same angle as the chosen 3D views to ensure similarity. The next step involves adding entry points and guide wires to these images. To automate this process, software is developed that places pins and torii based on the implant position and length. DRR's are created of these pins and torii in the lateral, inlet, and outlet view, the three most used fluoroscopic views. The DRR's are cropped and populated into the slideshow template. A series of DRR images is prepared for the perioperative process.

The slideshow with the preoperative VSP visualisation for each of the five patients was examined and checked to ensure correctness of the created images and patient data.

3.2.4 Perioperative VSP visualization

The process for perioperative visualisation of the VSP on top of CF as mentioned in Chapter 2 is optimised using the same Python scripting module. A graphical user interface is created which is used to load the intraoperative image and guide the registration of the DRR. A deep learning (DL) model was trained to perform the registration process. Training of the model was performed on DRR images that were created from pelvic CT scans. These were obtained from a subset of the CTPelvic1K database, known as the CLINIC database, which contains 103 CT images of healthy patients [58]. Six CT scans were exlcuded deu to lo quality. To prepare the CT data, it is centred at the S1 sacrum and the pelvic is aligned in true lateral. Using the aligned CT scans, four databases of DRR images, each containing 48,5k images, are developed using two different algorithms: a ray casting algorithm from the ITK insight toolbox [46] and a DL based algorithm [57]. These databases are used to train single stream convolutional networks and dual stream convolutional networks. A single stream convolutional network has been explored by others and presented promising

results [51]. Dual steam networks have been proposed before to obtain information from two images or do comparisons [59, 60]. The PyTorch (version 1.14.0) framework is used for the implementation of these networks. Appendix C contains the detailed description of the different steps to obtain the trained DL model.

To validate the models during training the accuracy was measured using a custom function that determines the percentage of predictions with an error less than 0.5 degrees from the ground truth. Although not experimentally verified, the average error for the manual process as mentioned in Chapter 2 was expected to be around 0.5 degrees. Additionally, for the best performing network heat maps are produced at different layers of the network to analyse the learned features and identify important factors that determine the model's output. These heat maps allow for the visualisation of the network's internal representations, which can be used to interpret the model's decision-making process.

3.3 Results

The proposed workflow was tested by an experienced user on CT scans from five different patients. The average time spent on the preoperative steps for VSP creation was reduced by 44 ± 7.8 % compared to the manual workflow. The creation time for the segmentations was reduced by 32 ± 6,9 %. The largest reduction in time was seen in the implant positioning part of the workflow with an average of 61 ± 11%. Fig. 3.1 shows the average creation time for each part. The total planning time was reduced from an average of 96 minutes to 50 minutes.

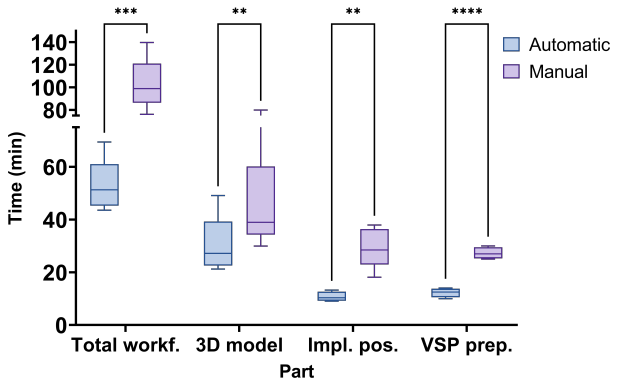

Figure 3.1: Box plot of the creation time for the individual steps of the virtual surgical planning comparing the automatic workflow to the manual workflow. Statistical significance between each workflow was tested with a paired t-test. Significance: (**) $P \geq 0.01$, (***) $P \geq 0.001$.

3.3.1 3D model creation

All CT scans were successfully segmented. The average time needed was 30 and 45 minutes for automatic and manual segmentation respectively. The paired t test showed the time reduction of 15 minutes to be significant (p = 0.019). In both instances, most time was spent on the manual hole filling step. The largest volume difference was 13.9 cm^3, with an average of 7.4 ± 4.8 cm^3. The average hausdorff distance between the 3D volumes was 0.34 mm. Fig 3.2 shows the spread of the mean hausdorff distance and volume difference for all the patients. Fig. 3.3 shows the hausdorff distance heatmaps, with problematic areas around the sacrum, hip joints, and in situ implants. The inexperienced user created the 3D models in 61 minutes using the manual workflow and in 35 minutes using the automated workflow.

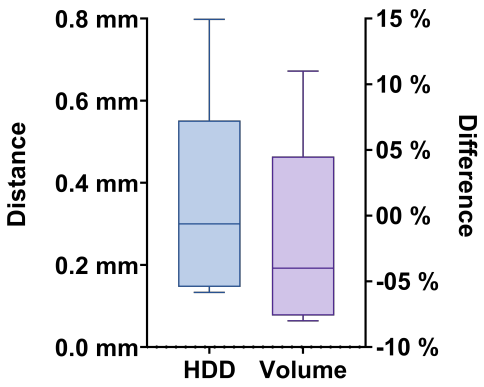

Figure 3.2: Box plot the mean hausdorff distance (HDD) and volume difference between the manual and automatically created models.

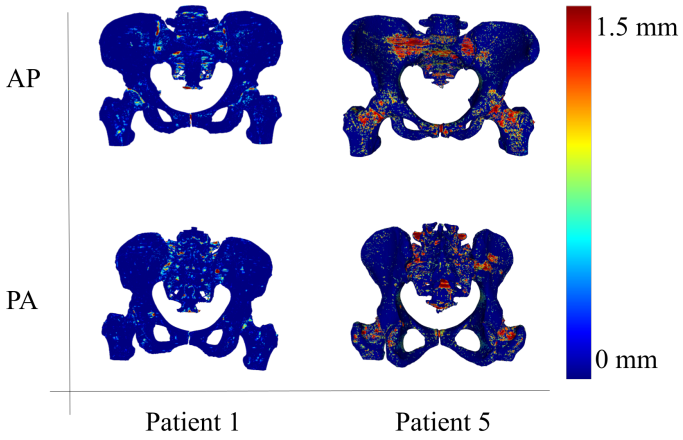

Figure 3.3: The hausdorff distance shown for the first and fifth patient, left and right respectively. Here the hausdorff distance is plotted onto the manually segmented model in the anterior-posterior view (AP, top row) and posterior-anterior view (PA, bottom row). The fifth patient (right) did have iFuse implants in the right SI joint.

3.3.2 Implant positioning

Creation of the VSP from the 3D models took on average 29 ± 7.7 min and 11 ± 1.8 min for the manual and automatic workflow respectively. For the inexperienced user, the VSP was created in 32 min and 16 min using the different workflows. The largest difference between the two workflows, besides the time reduction, was the ease of use. Following the protocol was simplified by reducing the number of steps (e.g. loading and renaming of implants) and prompting the user with the next step

3.3.3 Preoperative VSP visualization

The automatically created VSP visualisations were created on average 15 ± 0.8 min faster compared to the manual creation. In addition, the created visualisations showed a high degree of similarity in terms of image size and placement in the slideshow, whereas in the manually created visualisations, there was a more variation. In addition, the lateral view as used for the planning of the implants varied slightly from the angle used to create the lateral DRR for the manually created visualisations.

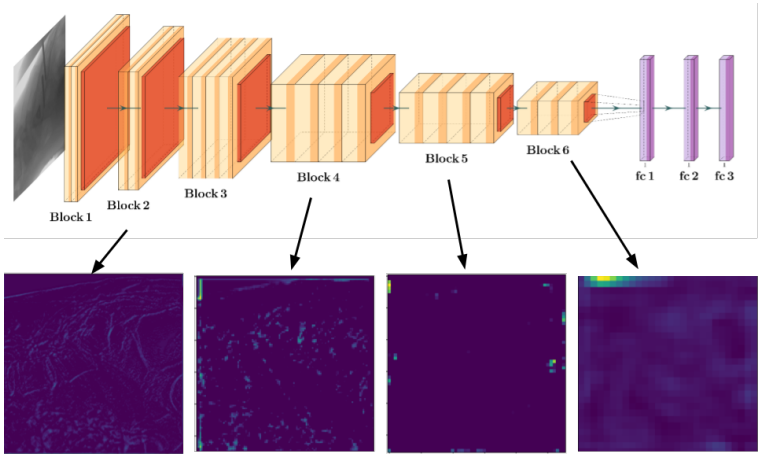

Figure 3.4: Schematic overview of the deep learning network (top) with heatmaps (bottom) of the best performing single stream network. Heatmaps are created from layer 10, 17, 27, and 40 from left to right respectively.

3.3.4 Perioperative VSP visualization

The deep learning model was trained to perform the registration process of the intraoperative image with a virtually created radiograph, a DRR, of the preoperative CT scan. For the image registration, the model determines the creation parameters from a single intraoperative x-ray image. The parameters consist of the rotation of the patient along the sagittal and longitudinal axis in degrees. The best performing network was able to detect these angles with a mean accuracy of 1.36 degrees on the validation dataset with 37% of the images scored with an error less than 0.5 degrees. The effects the different kinds of pretrained models is shown in fig. 3.5. It was trained on a dataset from 97 CT scans. This network consisted of a single stream model with a VGG19 pretrained feature extraction part. Heatmaps of various layers from this model are presented in fig. 3.4, showing that some anatomical structures are highlighted in the tenth layer heatmap, especially the edges of vertebrae four and five. However, in succeeding heatmaps, the left upper corner is highlighted as most important part of the image and there is no useful anatomical information here. The low percentage of predictions meeting the required error threshold, along with the heatmaps implying overfitting, indicated that this model is unsuitable for clinical use.

The best performing double stream network detected the beforementioned angles with a mean accuracy of 1.56 degrees with 21% of the images meeting the maximum error of 0.5 degrees. Each part of the dual stream network consisted of an Efficiency Net B7 pretrained feature extraction part.

3.4 Discussion

The use of VSP for SIJF has become the established clinical standard at our hospital. However, manual VSP creation remains time-consuming and susceptible to observer error. This study aimed to develop a (semi-)automated workflow and compare its performance to the previous manual approach. The results showed that the automated workflow significantly reduced the average time required to obtain a VSP and its preoperative visualization from a CT scan. Furthermore, in feedback provided by inexperienced user, the automated workflow was reported to be more user friendly. In the context of intraoperative VSP registration, multiple DL models were trained and evaluated. Among these models, the best performing one achieved an absolute angle error of 1.4 degrees on the validation dataset. Of these images, 63% were registered with an error larger than the clinical limit of 0.5 degrees. In addition, when analysing heatmaps depicting the decision-making process, it was observed that the model did not effectively learn the important features. The low percentage of predictions meeting the required error threshold, along with the heatmaps implying overfitting, indicated that this model is unsuitable for clinical use.

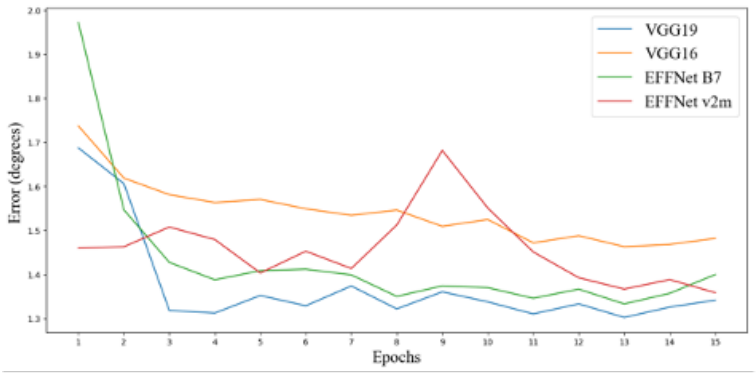

Figure 3.5: Experimental results of the effect the different pretrained modesl on the validation data set error. Here the single stream network is used and trained with 50% of the dataset. During training no data augmentation was used.

The widespread implementation of automated VSP creation in clinical practice is driven by its ability to reduce interobserver variability, planning time, and overall cost [61–65]. These automated workflows have been reported to produce VSP's that are suitable for clinical use. Carrillo et al. conducted a comparative study on planning time and reported a 35% decrease when implementing their (semi-)automatic workflow, which is consistent with the findings of the present study [61]. Furthermore, fully automatic workflows have demonstrated the capability to create VSPs within minutes [64, 66]. However, achieving fully automated and accurate VSP creation may not always be feasible. In the field of SIJF, the presence of high anatomical variation does affects implant placement [67, 68]. Therefore, some degree of input is still required for accurate implant positioning. On the other hand, creating the 3D models does not require manual input. Several researchers have proposed methods for fully automated pelvic segmentations, including statistical shape models [69–71] and more recently, DL-based approaches [54, 58, 72, 73]. These methods have the potential to further reduce VSP creation time. However, incorporating them into routine clinical care presents challenges.

Intraoperative use of the VSP during SIJF is often accompanied with computer-assisted surgery employs tracking of the C-arm or O-arm, the pelvis, and surgical tools [20, 24, 33–35]. However, our workflow focuses on utilizing VSP during surgery without the incorporation of additional tracking devices. Kordon et al. proposed a workflow for creating and superimposing VSP onto fluoroscopic images during reconstructive knee surgery [74]. While their focus lies in generating VSP after obtaining the fluoroscopy image, anatomical registration still plays a crucial role. They developed a DL-based method for anatomical keypoint detection, which yielded promising results. However, some error remained in this registration method, necessitating manual adjustments of key points. Although this method could be relevant for the registration process in SIJF, detecting anatomical landmarks of the pelvis in the lateral view has proven to be challenging [75]. While our current workflow primarily emphasizes VSP creation and visualization, the evaluation of surgical performance is not assessed. Bataeva et al. proposed a method for detecting guide wires from intraoperative fluoroscopy views [76]. Their approach estimated the 3D position of the guide wires using antero-posterior and lateral views with an accuracy of 1.9 $\pm$ 1.6 mm and 1.8 $\pm$ 1.3°. In the context of SIJF, where even small deviations can have significant impacts, such a method would require double the current accuracy to be clinically relevant.

One of the notable strengths of our current automated workflow is its implementation in CE marked software, ensuring its feasibility for clinical use. Throughout the development process, extensive testing on multiple SIJF cases has yielded consistently results. Furthermore, the workflow incorporates safety measures to minimize human errors. An example of such safety measure includes the selection and saving of the affected side, which is then maintained throughout the various steps of VSP creation. This prevents observers from segmenting or inserting implants in the incorrect SI joint, DRRs from the wrong side, or creating inaccurate VSP descriptions. Another significant safety measure is the automatic verification of

implant positioning. The workflow automatically ensures that implants are always planned parallel to each other, an important requirement for SIJF VSP. Additionally, the inter-implant distance is calculated. This distance is essential for preparing the "Variable Parallel Pin Guide" utilised during surgery. If the calculated inter-implant distance deviates from what is feasible with the guide, the user is alerted with an error and prompted to adjust the implant positioning. These safety measures enhance the feasibility of the workflow, particularly for inexperienced users. This was confirmed when evaluated by the inexperienced user.

The main benefit of the proposed perioperative registration process is its widespread applicability. The method to obtain the registration model is not case specific, allowing for easy implementation in both the inlet and outlet views. This would involve creating a new DRR database using the same CT scans and subsequently retraining the model. Moreover, beyond SIJF this method could be utilized in a range of surgical procedures. The only prerequisites are a preoperative 3D scan (e.g. CT and MRI), an intraoperative fluoroscopic image, and a VSP. It can solve the problem of needing specific views during surgery such as the lateral view in reconstructive knee surgery while using VSP [77]. The second strength of the method involves the validation of the deep learning model. The implementation of DL models into routine clinical care often encounters challenges related to the "black box" phenomenon, where the decision-making process of the model is not fully understood, leading to limited trust in its predictions. Therefore, a crucial aspect of this research was to visualize the decision-making process of the model using heatmaps. This visualization can contribute to the successful implementation of the model in clinical practice, as it enhances the understanding and trustworthiness of the model's predictions. In addition, the evaluation metrics were addressed to improve the evaluation. This evaluation metric is commonly reported as the average error or mean squared errors, which provide limited information about outliers. To address this limitation, a custom accuracy function was employed to demonstrate the model's proficiency in meeting a clinical requirement, in this case it was set at 0.5 degrees. This approach allows for a more comprehensive assessment of the model's performance, focusing on its ability to meet the specific clinical threshold rather than relying solely on average error metrics.

The major limitation of the (semi-)automatic workflow are the manual steps needed to create the 3D models. These manual steps are identical to those employed in the fully manual workflow and account for the observed differences in surface and volume of the 3D models between the two workflows. The 3D models are needed for the visualizing the pelvic in the DRRs. Consequently, the observed difference of 7.4 $\pm$ 4.8 cm^3 in volume and a low mean Hausdorff distance do not bear clinical significance. These differences reflect variability in manual operations rather than a shortcoming in the semi-automatic segmentation process. However, it should be noted that the cortical bone, which is depicted by the ala lines in the lateral view, undergoes distortion due to the presence of in situ iFuse implants. This is indicated in the heatmaps, illustrating the problematic areas for patient three and five. Nevertheless, this distortion is not amplified by automating and does not yield clinically discernible differences in the VSP visualizations.

A notable drawback of the proposed intraoperative registration method is its inadequate performance for clinical utilization. The best performing model demonstrated an absolute angle error of 1.4°. To interpret this error, it is imperative to consider the dataset creation process. The dataset was generated with a gaussian distributed range in angles with a standard deviation of $\pm$ 5°, with the mean centred at 0°. Consequently, if the model predicts randomly, the average error would be approximately 2.5°. Therefore, the model only exhibits 1.1° of learning. Most probably, this learning does not stem from the detection of specific anatomical structures, as indicated by the network's heatmaps. The primary contributing factor to the limited learning capabilities and rapid overfitting is the small variation within the database. For each patient, 500 DRRs are generated within a range of approximately -7° to +7° for both angles, resulting in the production of mostly similar images. While random data augmentation can partially mitigate the generation of similar images, it has proven insufficient in preventing overfitting. Expanding the database by incorporating more patients and creating fewer DRRs per patient could yield a more balanced dataset.

In order to overcome these limitations, future studies should consider the implementation of a fully automatic segmentation method, which should undergo extensive testing before clinical deployment. For improving the intraoperative registration, two potential approaches warrant investigation. Firstly, the exploration of unsupervised registration methods for 2D-to-2D registration can be pursued. By conducting

registration on a range of DRRs, the DRR that achieves the best registration with the intraoperative image can be determined. Alternatively, keypoint-based DL registration can be employed for 2D-to-2D registration. This approach offers the advantage of visualizing the image registration process and the identified keypoints. Such visualization is critical in intraoperative scenarios where trust in the software is essential and manual verification of the registration process is challenging. Furthermore, as an extension of the current workflow, the intraoperative component of the software can be expanded to incorporate surgical evaluation. This would facilitate real-time feedback and allow for adjustments of the surgery, therefore possibly enhancing the execution of VSP.

Despite possible improvements, already in its current stage, the presented approach represents a valuable tool for facilitating VSP for SIJF. Annually, our hospital alone conducts approximately 30 SIJF procedures, with VSP construction playing a crucial role in these interventions. The automation of this process has significantly decreased dependence on individual operators and improved adherence to the established protocol. This advantage is particularly significant for operators with limited experience in constructing SIJF VSPs. Moreover, the reduction in the time required for VSP creation enhances accessibility and decreases the associated costs of surgical preparation.

3.5 Conclusion

The manual VSP creation for SIJF, which is the clinical standard in our hospital, is time consuming and can be prone to observer error. Therefore, a new (semi)-automated workflow was developed. This workflow generated clinically equivalent 3D models and safe virtual surgical plannings in significantly less time. With the major benefit of improving adherence to established protocols. Some steps, such as the segmentation, still require manual input. Future research should focus on automating these steps, for example by utilizing deep learning models. Nevertheless, the current (semi)-automated workflow for virtual surgical planning for sacroiliac joint fusion is suitable for standard clinical care. A method to automatically perform the intraoperative image registration was developed to improve the (semi)-automated workflow. The developed method was able to estimate the angle at which the image was created. However, the accuracy of this method did not meet the required threshold for clinical use. The first steps in developing a suitable workflow were executed, more development is needed to improve this process before clinical implementation.

4

Clinical Validation of Visualising the Virtual Surgical Planning during Sacroiliac Joint Fusion

Abstract

Introduction - Within the guidelines of MDR and ISO, a workflow for (semi)-automated intraoperative visualization of virtual surgical planning during sacroiliac joint fusion surgery was developed and preclinically evaluated. This study investigated whether incorporating perioperative visualization could enhance implant accuracy during sacroiliac joint fusion surgery. A retrospective cohort, without perioperative visualization, was compared to a prospective cohort with real-time visualization of the planning.

Method - The retrospective cohort included all patients who underwent primary sacroiliac joint fusion surgery in 2022. All patients who underwent primary sacroiliac joint fusion surgery in June 2023 were included in the prospective cohort. In both cohorts, a virtual surgical planning was created and visualized intraoperatively. In the prospective cohort, the planning was registered and visualised on top of the perioperative image, for the lateral, inlet, and outlet views. Postoperative CT scans were used to evaluate implant accuracy and surgical metrics were compared between the two cohorts.

Results - A total of 29 patients were included in the study, with 24 in the retrospective cohort and 4 in the prospective cohort. In the retrospective cohort, the implant accuracy was 4.78 $\pm$ 1.31 mm for the tip of the implant and 4.17 $\pm$ 1.80° for the direction of the implant. The prospective cohort showed a significant improvement of 1.07 $\pm$ 0.42° ($P = 0.022$) in the average angle error compared to the retrospective cohort. No significant improvement was seen in implant accuracy based on the tip position.

Conclusion - This study successfully demonstrated the feasibility of intraoperatively registering and visualizing the virtual surgical planning on top of the lateral, inlet, and outlet views. Although the results show promising trends towards improved implant accuracy, the retrospective cohort size was insufficient to establish a statistically significant difference in surgery metrics. Further research with a larger sample size is needed to validate the potential improvement in reproducing the virtual surgical planning.

4.1 Introduction

SI joint fusion (SIJF) has been an option for the final treatment for SI joint dysfunction since it was first described in the 1920s [78]. However, there is ongoing debate regarding its efficacy [79]. Open surgery is traditionally highly invasive and associated with a high rate of non-union and low patient satisfaction [78]. In recent years, minimally invasive surgical (MIS) techniques for SIJF have been developed, with the first reported cases dating back to 2008 [2]. Although there are no reported randomised controlled trials, these techniques have shown significantly higher satisfaction rates ranging from 71% to 100% [79]. Despite the improvements in surgical outcomes, controversy remains regarding the efficacy of surgical treatment for SI joint dysfunction [79–82]. To address this controversy randomised controlled trials comparing MIS with non-surgical treatment have demonstrated superior outcomes with MIS [36, 83, 84].

Virtual surgical planning (VSP) has been implemented to improve the accuracy and safety of SIJF. VSP allows for optimal placement of implants, potentially resulting in improved stability and, therefore, better patient outcomes [10–12]. Furthermore, it enables assisted intraoperative guidance such as computer-assisted surgery (CAS). Tracking devices and robotic arms have been explored for guidance during SIJF. Although some studies have demonstrated a decrease in mispositioning with CAS [6, 85], others have not found a significant difference in accuracy compared to recreating the VSP [20, 24]. Additionally, when comparing conventional fluoroscopic (CF) guidance to CAS, the CF group does not include preoperative VSP creation, which alone could aid in safe implant placement. Besides CAS, patient-specific drill guides have been shown to safely guide screws into the spine and allow more accurate VSP recreation than free-handed screw placement[86, 87]. However, the need for bone preparation to fit the drill guide and distinct bone curvature for bone seating make this solution less suitable for SIJF. Because of the low cost and availability, CF guidance is still considered standard clinical care in SIJF and spine surgery [88].

To combine the benefits of the VSP with CF, chapters 2 and 3 detail a feasible workflow for perioperative visualisation, consisting of visualising the VSP on top of CF to optimise implant placement during SI joint fusion surgery. This has involved the automation of the VSP preparation within MDR and ISO guidelines and testing the pipeline. These pilot studies suggested that perioperative visualisation of the VSP is a low-cost and easily implementable solution without expensive CAS devices. Clinical evidence is needed to determine the advantages of this addition to the standard VSP use for SIJF.

This study aimed to evaluate the added value, based on implant accuracy, of perioperative visualisation of the VSP during SIJF. It is hypothesised that perioperative visualisation would result in improved accuracy of VSP reconstruction, as well as reduced operating time and radiation exposure. To test this hypothesis, the accuracy of VSP reconstruction with perioperative visualisation is compared to a retrospective cohort without perioperative visualisation.

4.2 Methods

4.2.1 Study design

The construction and use of VSP in SI joint fusion surgery have become standard clinical care since November 2021 in Medisch Spectrum Twente (MST, Enschede, The Netherlands). The ethical committee of MST gave a non-WMO declaration in July 2022 for research where 3D technology, including VSP, was used as standard care (3Database study). All patients who underwent primary SI joint fusion surgery in 2022 were included in the retrospective cohort of standard VSP, fig. 4.1 shows an overview of the inclusion procedure. Patients treated before July 2022 are included retrospectively and exempt from informed consent. Informed consent was obtained from patients treated after July 2022. The perioperative visualisation was added to the VSP clinical workflow in May 2023. All patients who underwent primary SI joint fusion surgery in June 2023 were prospectively included in the perioperative visualisation cohort. Implants that were not planned lateral and therefore not parallel to the other implants were excluded from analysis.

4.2.2 Procedure

The retrospective cohort in this study received standard SIJF surgery, which involves obtaining a preoperative CT scan, creating a VSP, creating the VSP visualisation preoperatively, and performing the surgery. During the surgical procedure, a slideshow consisting of lateral, inlet, and outlet DRRs of the VSP was presented to the surgeon. These images served as a reference for the placement of guide pins to facilitate the insertion of iFuse implants. In the prospective cohort, the preoperative planning was expanded with the creation of a range of lateral DRRs, as discussed in Chapter 2. The software used for this study was created entirely using medical software. In addition to the lateral DRR's the planning was also extended for the inlet and outlet views. During the surgical procedure, the optimal lateral, inlet, and outlet DRR was selected using the software and registered onto the fluoroscopic images. These fluoroscopic images with the VSP superimposed served as the reference for the surgeon during the placement of guide wires. The subsequent step of inserting the iFuse implants over the guide wires followed standard protocol in both cohorts.

4.2.3 Analysis

Patient characteristics (age, sex, BMI, left or right-sided SIJFs), operation characteristics (operating time, radiation time, radiation dose), the VSP, and CT scans were taken from the electronic health record. To analyse the added value based on the surgeon's perspective, the surgeon was asked to provide comments on the added benefit of the software. The postoperative CT scan is matched with the VSP to analyse the implant placement accuracy using Materialise Mimics 23.0 and 3-Matic 15.0 (Materialise, Leuven, Belgium). The implant placement accuracy is calculated based on a previously described method [89] and is defined as the deviation in planned and achieved apex position (total distance, x-, y-, and z-direction) and implant angle (total, xy-, and- yz-plane). The resulting variables are presented in a boxplot. The operating characteristics are compared between the two cohorts. Independent t-tests are performed to determine statistical differences in implant accuracy, patient and operating characteristics, and intraoperative complications between the two cohorts using SPSS version 28 (SPSS Inc., Chicago, USA). The patient's BMI is a confounder for the radiation dose and time. Therefore, a multivariate logistic regression test is performed to correct for the BMI.

4.3 Results

Twenty-eight interventions were included in total, of which 24 in the retrospective cohort and 4 in the prospective cohort (see fig 4.1). The cohort characteristics are shown in tab. 4.1. Due to the limited number of interventions in the prospective cohort, no statistical tests were performed on the surgery characteristics. For the surgery evaluation, no difference was observed for the mean implant position of the tip. A significant reduction in implant angle error was observed, from $4.35 \pm 2.01^\circ$ for the retrospective cohort to $3.28 \pm 1.18^\circ$ for the prospective cohort ($p = 0.022$).

The surgeon commented that the workflow for intraoperative visualisation is fast enough for clinical use. In addition, the representation of the VSP at the adjusted angle provides crucial information to recreate the VSP accurately. There were some angular differences seen between the fluoroscopic views at the start of the operation (used for the VSP visualisation) and the final views used for inserting the implants.

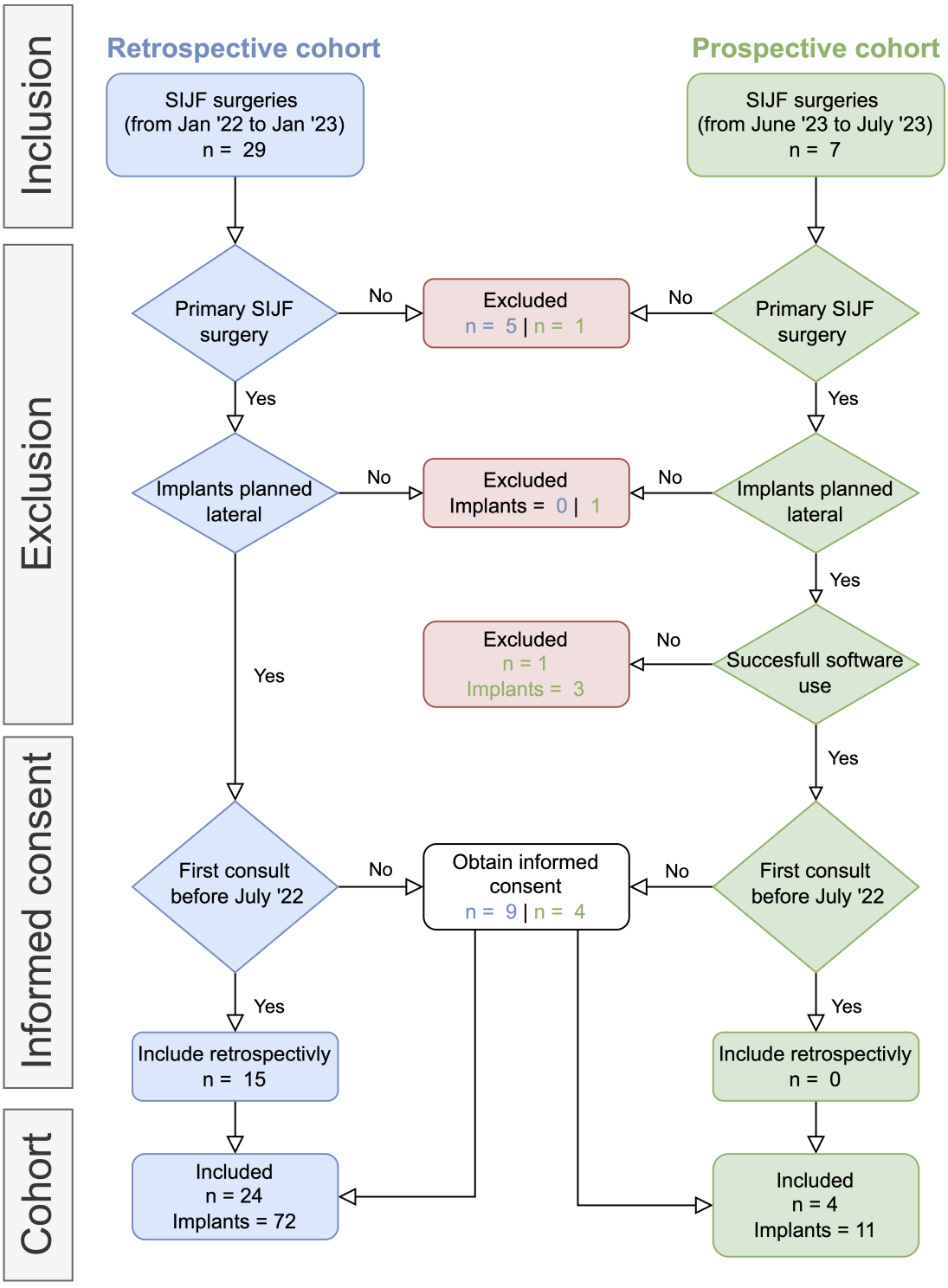

Figure 4.1: Flowchart of the inclusion of the retrospective cohort (left column) and the prospective cohort (right column). *n = number of patients.*

Table 4.1: Cohort characteristics.

PATIENT CHARACTERISTICS	**RETROSPECTIVE COHORT**	**PROSPECTIVE COHORT**
INTERVENTIONS (N)	24	4
IMPLANTS (N)	72	11
AGE (YEARS ± SD)	42 ± 10.8	50 ± 10.8
FEMALE (%)	96	100
BMI (KG/M^2 ± SD)	30.3 ± 5.84	26.9 ± 2.09
LEFT SIDE (%)	54.2	50.0
VSP CHARACTERISTICS		
MEAN IMPLANT LENGTH (MM ± SD)	47.4 ± 8.1	49.1 ± 6.7
SURGERY CHARACTERISTICS		
DURATION (MIN ± SD)	40.1 ± 7.84	40.3 ± 4.43
RADIATION DOSE (CGYCM2 ± SD)	(1.22 ± 0.380) *10^3	(0.742 ± 0.202) *10^3
RADIATION TIME (SECONDS ± SD)	33.0 ± 9.59	26.5 ± 5.80
SURGERY EVALUATION		
IMPLANT POSITION DEVIATION MEAN (MM ± SD)	4.77 ± 2.05	4.84 ± 1.59
IMPLANT POSITION DEVIATION MEAN OF MAX (MM ± SD)	6.25 ± 1.74	6.70 ± 0.70
IMPLANT ANGLE DEVIATION MEAN (° ± SD)	4.35 ± 2.01	3.28 ± 1.18
IMPLANT ANGLE DEVIATION MEAN OF MAX (° ± SD)	5.69 ± 1.80	3.90 ± 0.90

SD: Standard deviation, KG: Kilogram, M: Meter, MM: Millimeters, Min: Minutes, CGY: Centigray, CM: Centimeters, and ° Degrees

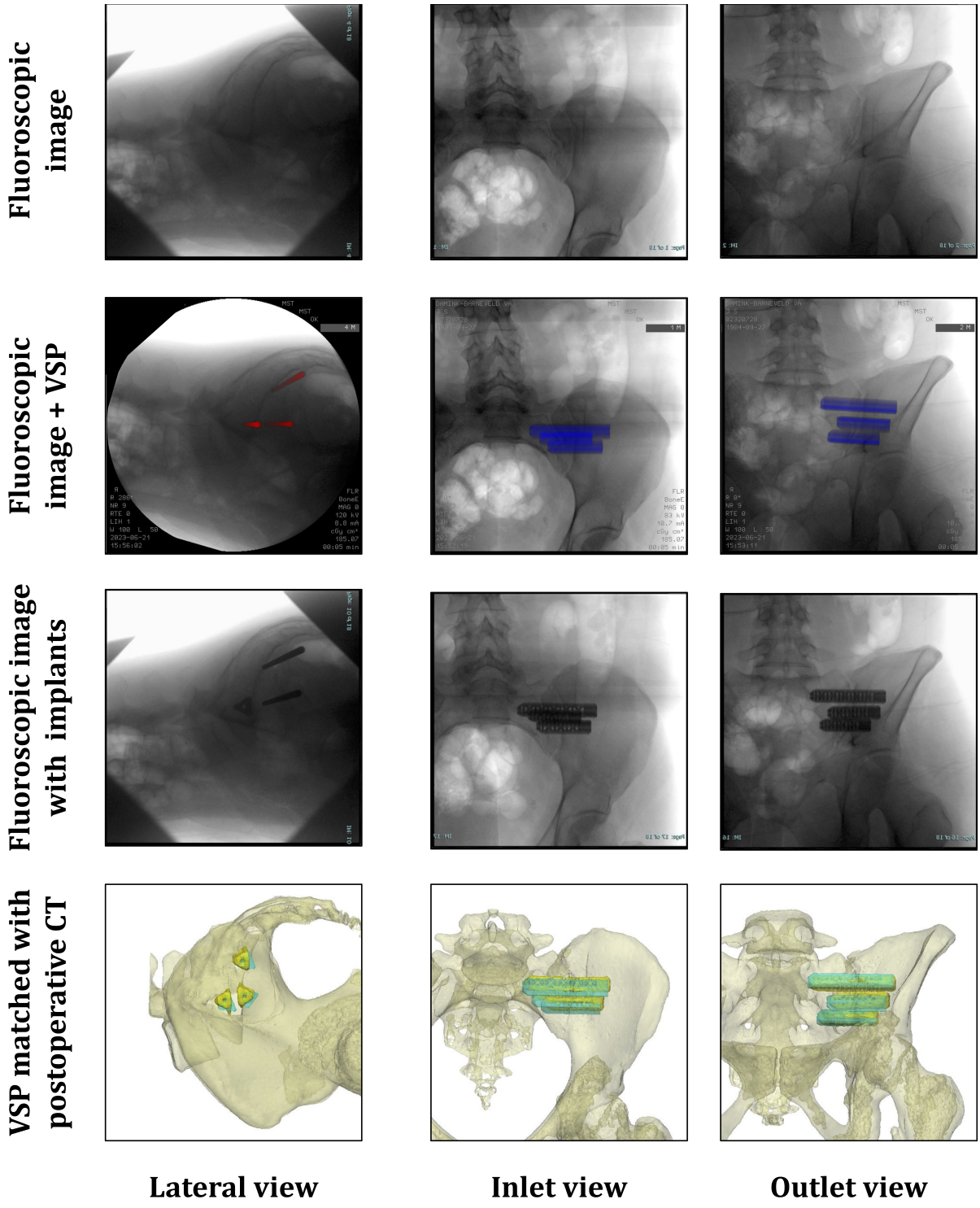

Figure 4.2: Intraoperative images for patient one in the top three rows. In the second row, the virtual surgical planning (VSP) is superimposed on top of the intraoperative image. In the lateral view, the planned guide pins are shown in red. In the inlet and outlet views, the planned implants are shown in blue. The bottom row shows the planned implants (in cyan) and the postoperative implant positioning (in yellow) for patient one.

4.4 Discussion

Recreating the VSP during SIJF is crucial for achieving optimal implant positioning and preventing complications. The developed workflow aimed to improve implant accuracy by incorporating perioperative visualisation. A retrospective cohort with standard virtual surgical planning was compared to a prospective cohort where planning was visualised on top of perioperative images. The results showed a significant difference of $1.07 \pm 0.42°$ in implant angle accuracy, favouring the cohort with the perioperative visualisation ($p = 0.022$). These findings suggest that visualizing the virtual surgical planning on top of perioperative images could be beneficial during SIJF.

The intraoperative complication rate for SIJF is generally low, with reoperation rates ranging from 0 % to 9.1% and an average of 2.9% according to a review by Heiney et al. [37]. In our study, no intra operative complications were observed. Literature lacks reports on implant accuracies based on VSP to postoperative CT scan comparisons for SIJF. Nevertheless, studies on other procedures such as pedicle screw placement have reported entry point deviations of 1.40 ± 0.81 mm and 3D angular deviations of $6.70 \pm 3.77°$ [90]. These errors affect the accuracy of the implant tip, which is believed to be comparable to the error observed in the tip position in our study. However, it should be noted that the angular implant accuracy in our study was lower in both cohorts. Certain navigation techniques, such as O-arm navigation, are expected to increase radiation dose by approximately 40 seconds of fluoroscopy [91]. In our study, the increased guidance in the prospective cohort did not result in additional radiation dose. Direct comparison to other techniques is challenging due to differences in reported metrics. Wang et al. reported a radiation exposure of 13.7 ± 6.2 mGy when using robotic navigation, which, with certain assumptions, would correspond to a DAP of 856 ± 398 cGycm^2 with comparable BMI [92]. This DAP is comparable to the prospective cohort in our study.

The major strength of this research lies in the clinical comparison of the workflow. The comparison between the two cohorts was based on quantitative surgical outcome measures, and the surgeries were performed by a single surgeon, allowing for a robust evaluation of the added benefit of the new workflow. However, a limitation of this study is the low number of cases in the prospective cohort. Power analysis indicated that a prospective cohort of 14 patients would be required to detect a 400 cGycm^2 reduction in mean error as significant. The initial target of including at least 14 patients was not feasible within the duration of the study, as there were fewer operations than expected during the inclusion period. Another limitation is the lack of direct translation to clinical benefits. Surgical outcomes in terms of complications were comparable between the cohorts. Whether better VSP recreation leads to improved patient outcomes remains unknown. Therefore, future studies should consider incorporating patient-reported outcomes to assess the clinical benefits of accurately reproducing the VSP.

Although the direct clinical benefits have not been proven yet, it is anticipated that better recreation of the VSP can allow for smaller safety margins during VSP creation. Consequently, implants can be positioned in a more stable configuration, such as further apart or in a diverging pattern [10, 11, 43]. Additionally, there was no increase in the cost of surgery due to longer operation times or expensive devices. In addition, the operation time could lower with a more optimized or automatic workflow. A small clinical benefit could therefore be enough that it outweighs the extra work.

4.5 Conclusion

This study successfully demonstrated the feasibility of intraoperatively registering and visualising the virtual surgical planning on top of the lateral, inlet, and outlet views during SIJF surgery. The workflow can be implemented in the clinic without needing expensive devices due to the creation of CE-marked medical software. The results show promising trends towards improved implant accuracy. Radiation exposure of the retrospective cohort was lower, however the size of this cohort was insufficient to establish a statistically significant difference. Surgical time was comparable in both cohorts. Further evaluation in a larger prospective cohort is needed to determine whether there is the significant difference in implant accuracy remains. Moreover, it is important to investigate whether the potential added accuracy can translate into better patient outcomes.

5
General Discussion

SI joint dysfunction is the cause the debilitating pain for many patients with low back pain. When conservative treatment options no longer suffice, SIJF has demonstrated favourable outcomes. During SIJF, it is crucial to avoid closely located nerve structures. Expensive tracking devices have been used to guide the insertion of the implants. However, CF remains the golden standard. Reproducing the pre-planned implant position using CF can be challenging. Therefore, the aim of thesis was to improve perioperative CF guidance by superimposing DRR onto the CF images during SIJF for patients with SI dysfunction.

Chapter 1 of this thesis has provided valuable insights into the use of CF during SIJF and SI screw placement. The literature examined in this chapter has presented conflicting information on this topic. Therefore, the significance of C-arm placement has been elucidated, emphasizing its clinical impact. Although CF is used to check the angle of the implant during surgery, this aspect was not considered during virtual implant placement. Therefore, a follow-up study could determine whether misplacing the C-arm indeed affects the clinical outcomes. Together with the knowledge gaps obtained through the questionnaire, the subsequent phase would involve determining the optimal method for informing and training current and future surgeons. Knowledge obtained on the use of CF during SIJF could potentially be extended to other fields where CF is employed. One such field is pedicle screw placement in spine surgery, where precise guidance is crucial, as deviations greater than 5° can lead to complications [93].

Chapter 2 provided a comprehensive description of the proposed workflow for superimposing the VSP onto the CF image. The software was developed and able to successfully visualize the VSP onto the CF image. The manual workflow was fast and accurate enough during clinical testing. However, clinical application into routine care of the fully custom software outlined may not be feasible within the MDR guidelines.

Chapter 3 has highlighted the effects automation can have on a clinical workflow. The strength of the developed workflow is its direct implementability into routine clinical care. In addition, it demonstrated clear time-saving benefits. However, it is essential to consider that the process of developing the automation script itself can be time-consuming. Consequently, it may not be suitable or time-effective to automate every clinical workflow, especially in cases where demand is low and manual intervention remains necessary. It is important to note that the implementation of automated workflows inherently restricts the ability to deviate from the established protocol. In the context of patient-specific planning, this can often be the case, making it challenging to incorporate every possible variation into the automation script. During the implementation of this workflow this should be taken into consideration. Automating the workflow further was attempted by training DL models. While the convolutional DL models discussed in Chapter 3 demonstrated fast processing times, they were found to be inaccurate in 63% of the cases. Further development of such workflow should therefore involve different DL methods.

Chapter 4 of the thesis aimed to address the major limitations identified in Chapter 2 by conducting a comparison to standard surgery and evaluating multiple cases. Although no significant difference in accuracy was observed, it is important to consider that the limited number of cases analysed in this study may have influenced the findings. Therefore, further clinical implementation and evaluation are crucial to fully ascertain the potential benefits of intraoperative visualization.

To conclude, improving perioperative CF guidance by superimposing DRR onto the CF images can be beneficial during SIJF, but a larger clinical trial is needed to confirm. In addition, an automatic registration workflow as described in chapter 3, could be implemented in various surgeries that rely on CF and could revolutionize the use of the standard C-arm.

Bibliography

[1] A. Kiapour, A. Joukar, H. Elgafy, D. U. Erbulut, A. K. Agarwal, and V. K. Goel, "Biomechanics of the sacroiliac joint: Anatomy, function, biomechanics, sexual dimorphism, and causes of pain," *International Journal of Spine Surgery*, vol. 14, pp. S3–S13, 2 2020.

[2] A. G. Smith, R. Capobianco, D. Cher, L. Rudolf, D. Sachs, M. Gundanna, J. Kleiner, M. G. Mody, and A. N. Shamie, "Open versus minimally invasive sacroiliac joint fusion: a multi-center comparison of perioperative measures and clinical outcomes," *Annals of Surgical Innovation and Research*, vol. 7, p. 14, 12 2013.

[3] H. Telli, S. Telli, and M. Topal, "The validity and reliability of provocation tests in the diagnosis of sacroiliac joint dysfunction.," *Pain physician*, vol. 21, pp. E367–E376, 2018.

[4] B. A. Zelle, G. S. Gruen, S. Brown, and S. George, "Sacroiliac joint dysfunction," *The Clinical Journal of Pain*, vol. 21, pp. 446–455, 9 2005.

[5] K. M. Szadek, P. van der Wurff, M. W. van Tulder, W. W. Zuurmond, and R. S. Perez, "Diagnostic validity of criteria for sacroiliac joint pain: A systematic review," *The Journal of Pain*, vol. 10, pp. 354–368, 4 2009.

[6] J.-Q. Wang, Y. Wang, Y. Feng, W. Han, Y.-G. Su, W.-Y. Liu, W.-J. Zhang, X.-B. Wu, M.-Y. Wang, and Y.-B. Fan, "Percutaneous sacroiliac screw placement," *Chinese Medical Journal*, vol. 130, pp. 2527–2534, 11 2017.

[7] S. Falowski, D. Sayed, J. Pope, D. Patterson, M. Fishman, M. Gupta, and P. Mehta, "A review and algorithm in the diagnosis and treatment of sacroiliac joint pain," *Journal of Pain Research*, vol. Volume 13, pp. 3337–3348, 12 2020.

[8] C. M. Matias, L. Velagapudi, T. S. Montenegro, and J. E. Heller, "Minimally invasive sacroiliac fusion—a review," *Current Pain and Headache Reports*, vol. 26, pp. 173–182, 3 2022.

[9] P. Whang, D. Cher, D. Polly, C. Frank, H. Lockstadt, J. Glaser, R. Limoni, and J. Sembrano, "Sacroiliac joint fusion using triangular titanium implants vs. non-surgical management: Six-month outcomes from a prospective randomized controlled trial," *International Journal of Spine Surgery*, vol. 9, p. 6, 1 2015.

[10] H. Soriano-Baron, D. P. Lindsey, N. Rodriguez-Martinez, P. M. Reyes, A. Newcomb, S. A. Yerby, and N. R. Crawford, "The effect of implant placement on sacroiliac joint range of motion," *Spine*, vol. 40, pp. E525–E530, 5 2015.

[11] N. Kampkuiper, F. Schröder, E. Hekman, M. Koenrades, and J. Nellensteijn, "Letter to the editor: "biomechanical stability of the sacroiliac joint with differing impact configurations in a synthetic model"," *International Journal of Spine Surgery*, p. 8360, 9 2022.

[12] C. Payne, S. Jaffee, I. Swink, D. Cook, M. Yeager, M. Oh, G. Schmidt, D. P. Lindsey, S. A. Yerby, and B. Cheng, "Comparative analysis of the lateral and posterolateral trajectories for fixation of the sacroiliac joint—a cadaveric study," *Journal of Orthopaedic Surgery and Research*, vol. 15, p. 489, 12 2020.

[13] D. M. Kahler, "Percutaneous screw insertion for acetabular and sacral fractures," *Techniques in Orthopaedics*, vol. 18, pp. 174–183, 6 2003.

[14] B. Schippers, E. Hekman, S. van Helden, M. Boomsma, J. van Osch, and R. Nijveldt, "Enhancing perioperative landmark detection during sacroiliac joint fusion in patients suffering from low back pain," *Computer Assisted Surgery*, vol. 26, pp. 41–48, 1 2021.

[15] R. Beckers, Z. Kwade, and F. Zanca, "The eu medical device regulation: Implications for artificial intelligence-based medical device software in medical physics," *Physica Medica*, vol. 83, pp. 1–8, 3 2021.

[16] D. Demetriades, M. Karaiskakis, K. Toutouzas, K. Alo, G. Velmahos, and L. Chan, "Pelvic fractures: Epidemiology and predictors of associated abdominal injuries and outcomes1," *Journal of the American College of Surgeons*, vol. 195, pp. 1–10, 7 2002.

[17] T. Dienstknecht, A. Berner, A. Lenich, M. Nerlich, and B. Fuechtmeier, "A minimally invasive stabilizing system for dorsal pelvic ring injuries," *Clinical Orthopaedics Related Research*, vol. 469, pp. 3209–3217, 11 2011.

[18] J. D. Piche, S. R. Muscatelli, M. A.-A. Waheed, R. D. Patel, and I. S. Aleem, "Robotic navigation system utilization for percutaneous sacroiliac screw placement: surgical setup and technique," *Journal of Spine Surgery*, vol. 7, pp. 197–203, 6 2021.

[19] R. Han, A. Uneri, T. D. Silva, M. Ketcha, J. Goerres, S. Vogt, G. Kleinszig, G. Osgood, and J. H. Siewerdsen, "Atlas-based automatic planning and 3d–2d fluoroscopic guidance in pelvic trauma surgery," *Physics in Medicine Biology*, vol. 64, p. 095022, 5 2019.

[20] J. Verbeek, E. Hermans, A. van Vugt, and J. P. Frölke, "Correct positioning of percutaneous iliosacral screws with computer-navigated versus fluoroscopically guided surgery in traumatic pelvic ring fractures," *Journal of Orthopaedic Trauma*, vol. 30, pp. 331–335, 6 2016.

[21] F. Gras, I. Marintschev, A. Wilharm, K. Klos, T. Mückley, and G. O. Hofmann, "2d-fluoroscopic navigated percutaneous screw fixation of pelvic ring injuries - a case series," *BMC Musculoskeletal Disorders*, vol. 11, p. 153, 12 2010.

[22] B. H. Ziran, A. D. Wasan, D. M. Marks, S. A. Olson, and M. W. Chapman, "Fluoroscopic imaging guides of the posterior pelvis pertaining to iliosacral screw placement," *Journal of Trauma: Injury, Infection Critical Care*, vol. 62, pp. 347–356, 2 2007.

[23] D. Rikli, S. Goldhahn, M. Blauth, S. Mehta, M. Cunningham, and A. Joeris, "Optimizing intraoperative imaging during proximal femoral fracture fixation – a performance improvement program for surgeons," *Injury*, vol. 49, pp. 339–344, 2 2018.

[24] J. Berger-Groch, M. Lueers, J. M. Rueger, W. Lehmann, D. Thiesen, J. P. Kolb, M. J. Hartel, and L. G. Grossterlinden, "Accuracy of navigated and conventional iliosacral screw placement in b- and c-type pelvic ring fractures," *European Journal of Trauma and Emergency Surgery*, vol. 46, pp. 107–113, 2 2020.

[25] G. Burström, M. Balicki, A. Patriciu, S. Kyne, A. Popovic, R. Holthuizen, R. Homan, H. Skulason, O. Persson, E. Edström, and A. Elmi-Terander, "Feasibility and accuracy of a robotic guidance system for navigated spine surgery in a hybrid operating room: a cadaver study," *Scientific Reports*, vol. 10, p. 7522, 12 2020.

[26] P. Giannoudis, G. Papadokostakis, K. Alpantaki, G. Kontakis, and B. Chalidis, "Is the lateral sacral fluoroscopic view essential for accurate percutaneous sacroiliac screw insertion?," *Injury*, vol. 39, pp. 875–880, 8 2008.

[27] R. E. Hilgert, J. Finn, and H.-J. Egbers, "Technik der perkutanen si-verschraubung mit unterstützung durch konventionellen c-bogen," *Der Unfallchirurg*, vol. 108, pp. 954–960, 11 2005.

[28] R. Banerjee, P. Brink, M. Cimerman, and a. M. T. Tim Pohlemann, "Iliosacral screw for si joint," https://surgeryreference.aofoundation.org/orthopedic-trauma/adult-trauma/pelvic-ring/basic-technique/iliosacral-screw-for-si-joint.

[29] M. L. C. Chip, P. T. Simonian, S. G. Agnew, and F. A. Mann, "Radiographic recognition of the sacral alar slope for optimal placement of iliosacral screws: A cadaveric and clinical study," *Journal of Orthopaedic Trauma*, vol. 10, pp. 171–177, 4 1996.

[30] C. Yi, S. Burns, and D. J. Hak, "Intraoperative fluoroscopic evaluation of screw placement during pelvic and acetabular surgery," *Journal of Orthopaedic Trauma*, vol. 28, pp. 48–56, 1 2014.

[31] A. Gänsslen, T. Hüfner, and C. Krettek, "Die bildwandergestützte, perkutane transiliosakrale schraubenfixation instabiler beckenverletzungen," *Operative Orthopädie und Traumatologie*, vol. 18, pp. 225–244, 8 2006.

[32] G. L. Schmidt, A. K. Bhandutia, and D. T. Altman, "Management of sacroiliac joint pain," *Journal of the American Academy of Orthopaedic Surgeons*, vol. 26, pp. 610–616, 9 2018.

[33] M. Arand, L. Kinzl, and F. Gebhard, "Computer-guidance in percutaneous screw stabilization of the iliosacral joint," *Clinical Orthopaedics and Related Research*, vol. 422, pp. 201–207, 5 2004.

[34] A. Matityahu, D. Kahler, C. Krettek, U. Stöckle, P. A. Grutzner, P. Messmer, J. Ljungqvist, and F. Gebhard, "Three-dimensional navigation is more accurate than two-dimensional navigation or conventional fluoroscopy for percutaneous sacroiliac screw fixation in the dysmorphic sacrum," *Journal of Orthopaedic Trauma*, vol. 28, pp. 707–710, 12 2014.

[35] R. Härtl, K. S. Lam, J. Wang, A. Korge, F. Kandziora, and L. Audigé, "Worldwide survey on the use of navigation in spine surgery," *World Neurosurgery*, vol. 79, pp. 162–172, 1 2013.

[36] S. P. Cohen, Y. Chen, and N. J. Neufeld, "Sacroiliac joint pain: a comprehensive review of epidemiology, diagnosis and treatment," *Expert Review of Neurotherapeutics*, vol. 13, pp. 99–116, 1 2013.

[37] J. Heiney, R. Capobianco, and D. Cher, "A systematic review of minimally invasive sacroiliac joint fusion utilizing a lateral transarticular technique," *International Journal of Spine Surgery*, vol. 9, p. 40, 1 2015.

[38] A. G. Shamrock, A. Patel, M. Alam, K. H. Shamrock, and M. A. Maaieh, "The safety profile of percutaneous minimally invasive sacroiliac joint fusion," *Global Spine Journal*, vol. 9, pp. 874–880, 12 2019.

[39] P. Grechenig, C. Grechenig, G. Hohenberger, M. J. Maier, G. Lipnik, A. Schwarz, T. di Vora, and A. Gänsslen, "Relation of the lumbosacral trunk to the sacro-iliac joint," *Scientific Reports*, vol. 11, p. 20211, 12 2021.

[40] J. S. Cheng and J. K. Song, "Anatomy of the sacrum," *Neurosurgical Focus*, vol. 15, pp. 1–4, 8 2003.

[41] M. K. Jesse, C. Kleck, A. Williams, B. Petersen, D. Glueck, K. Lind, and V. Patel, "3d morphometric analysis of normal sacroiliac joints: A new classification of surface shape variation and the potential implications in pain syndromes.," *Pain physician*, vol. 20, pp. E701–E709, 7 2017.

[42] N. K. Mahato, "Implications of structural variations in the human sacrum: why is an anatomical classification crucial?," *Surgical and Radiologic Anatomy*, vol. 38, pp. 947–954, 10 2016.

[43] A. L. Freeman, J. E. Bechtold, and D. W. Polly, "Biomechanical stability of the sacroiliac joint with differing implant configurations in a synthetic model," *International Journal of Spine Surgery*, vol. 15, pp. 853–861, 10 2021.

[44] P. Markelj, D. Tomaževič, B. Likar, and F. Pernuš, "A review of 3d/2d registration methods for image-guided interventions," *Medical Image Analysis*, vol. 16, pp. 642–661, 4 2012.

[45] S. Saadat, D. Perriman, J. M. Scarvell, P. N. Smith, C. R. Galvin, J. Lynch, and M. R. Pickering, "An efficient hybrid method for 3d to 2d medical image registration," *International Journal of Computer Assisted Radiology and Surgery*, vol. 17, pp. 1313–1320, 7 2022.

[46] J. Wu, "Itk-based implementation of two-projection 2d/3d registration method with an application in patient setup for external beam radiotherapy," *The Insight Journal*, 12 2010.

[47] M. A. Bollet, H. A. McNair, V. N. Hansen, A. Norman, U. O'Doherty, H. Taylor, M. Rose, R. Mukherjee, and R. Huddart, "Can digitally reconstructed radiographs (drrs) replace simulation films in prostate cancer conformal radiotherapy?," *International Journal of Radiation Oncology*Biology*Physics*, vol. 57, pp. 1122–1130, 11 2003.

[48] J. Montúfar, M. Romero, V. Muñoz-Jiménez, R. Scougall-Vilchis, and B. Jiménez, "Perspective and orthogonal cbct/ct digitally reconstructed radiographs compared to conventional cephalograms," 6 2018.

[49] P. H. Schönemann, "A generalized solution of the orthogonal procrustes problem," *Psychometrika*, vol. 31, pp. 1–10, 3 1966.

[50] C. J. Percival, J. Devine, B. C. Darwin, W. Liu, M. Eede, R. M. Henkelman, and B. Hallgrimsson, "The effect of automated landmark identification on morphometric analyses," *Journal of Anatomy*, vol. 234, pp. 917–935, 6 2019.

[51] L. Kausch, S. Thomas, H. Kunze, M. Privalov, S. Vetter, J. Franke, A. H. Mahnken, L. Maier-Hein, and K. Maier-Hein, "Toward automatic c-arm positioning for standard projections in orthopedic surgery," *International Journal of Computer Assisted Radiology and Surgery*, vol. 15, pp. 1095–1105, 7 2020.

[52] J. Wallner, M. Schwaiger, K. Hochegger, C. Gsaxner, W. Zemann, and J. Egger, "A review on multiplatform evaluations of semi-automatic open-source based image segmentation for cranio-maxillofacial surgery," *Computer Methods and Programs in Biomedicine*, vol. 182, p. 105102, 12 2019.

[53] G. Dot, T. Schouman, G. Dubois, P. Rouch, and L. Gajny, "Fully automatic segmentation of craniomaxillofacial ct scans for computer-assisted orthognathic surgery planning using the nnu-net framework," *European Radiology*, vol. 32, pp. 3639–3648, 6 2022.

[54] J. Wasserthal, M. Meyer, H.-C. Breit, J. Cyriac, S. Yang, and M. Segeroth, "Totalsegmentator: robust segmentation of 104 anatomical structures in ct images," *Cornell University, Arxiv*, 2022.

[55] J. Vicory, G. J. M. Garcia, J. S. Rhee, and A. Enquobahrie, "Toward automatic atlas-based surgical planning for septoplasty," *International Journal of Computer Assisted Radiology and Surgery*, vol. 17, pp. 403–411, 2 2022.

[56] D. Wagner, L. Kamer, P. M. Rommens, T. Sawaguchi, R. G. Richards, and H. Noser, "3d statistical modeling techniques to investigate the anatomy of the sacrum, its bone mass distribution, and the trans-sacral corridors," *Journal of Orthopaedic Research*, vol. 32, pp. 1543–1548, 11 2014.

[57] M. Unberath, J.-N. Zaech, S. chung Lee, B. Bier, J. Fotouhi, M. Armand, and N. Navab, "Deepdrr – a catalyst for machine learning in fluoroscopy-guided procedures," *Cornell University, Arxiv*, 2018.

[58] P. Liu, H. Han, Y. Du, H. Zhu, Y. Li, F. Gu, H. Xiao, J. Li, C. Zhao, L. Xiao, X. Wu, and S. K. Zhou, "Deep learning to segment pelvic bones: large-scale ct datasets and baseline models," *International Journal of Computer Assisted Radiology and Surgery*, vol. 16, pp. 749–756, 5 2021.

[59] J. Rubin, D. Sanghavi, C. Zhao, K. Lee, A. Qadir, and M. Xu-Wilson, "Large scale automated reading of frontal and lateral chest x-rays using dual convolutional neural networks," 4 2018.

[60] D. Toth, S. Miao, T. Kurzendorfer, C. A. Rinaldi, R. Liao, T. Mansi, K. Rhode, and P. Mountney, "3d/2d model-to-image registration by imitation learning for cardiac procedures," *International Journal of Computer Assisted Radiology and Surgery*, vol. 13, pp. 1141–1149, 8 2018.

[61] F. Carrillo, S. Roner, M. von Atzigen, A. Schweizer, L. Nagy, L. Vlachopoulos, J. G. Snedeker, and P. Fürnstahl, "An automatic genetic algorithm framework for the optimization of three-dimensional surgical plans of forearm corrective osteotomies," *Medical Image Analysis*, vol. 60, p. 101598, 2 2020.

[62] P. G. M. Knoops, A. Papaioannou, A. Borghi, R. W. F. Breakey, A. T. Wilson, O. Jeelani, S. Zafeiriou, D. Steinbacher, B. L. Padwa, D. J. Dunaway, and S. Schievano, "A machine learning framework for automated diagnosis and computer-assisted planning in plastic and reconstructive surgery," *Scientific Reports*, vol. 9, p. 13597, 9 2019.

[63] H. Li, J. Xu, D. Zhang, Y. He, and X. Chen, "Automatic surgical planning based on bone density assessment and path integral in cone space for reverse shoulder arthroplasty," *International Journal of Computer Assisted Radiology and Surgery*, vol. 17, pp. 1017–1027, 6 2022.

[64] A. Modabber, A. Rauen, N. Ayoub, S. C. Möhlhenrich, F. Peters, K. Kniha, F. Hölzle, and S. Raith, "Evaluation of a novel algorithm for automating virtual surgical planning in mandibular reconstruction using fibula flaps," *Journal of Cranio-Maxillofacial Surgery*, vol. 47, pp. 1378–1386, 9 2019.

[65] B. W. Starnes, B. Tatum, and N. Singh, "Procedural and perioperative results in patients treated with fenestrated endovascular aneurysm repair planned by automated software in a physician-sponsored investigational device exemption trial of physician-modified endografts," *Journal of Vascular Surgery*, vol. 68, pp. 1297–1307, 11 2018.

[66] J. Wallner, K. Hochegger, X. Chen, I. Mischak, K. Reinbacher, M. Pau, T. Zrnc, K. Schwenzer-Zimmerer, W. Zemann, D. Schmalstieg, and J. Egger, "Clinical evaluation of semi-automatic open-source algorithmic software segmentation of the mandibular bone: Practical feasibility and assessment of a new course of action," *PLOS ONE*, vol. 13, p. e0196378, 5 2018.

[67] R. Postacchini, G. Trasimeni, F. Ripani, P. Sessa, S. Perotti, and F. Postacchini, "Morphometric anatomical and ct study of the human adult sacroiliac region," *Surgical and Radiologic Anatomy*, vol. 39, pp. 85–94, 1 2017.

[68] C. Wu, Y.-C. Liu, H. Koga, C.-Y. Lee, P.-Y. Wang, D. Cher, W. C. Reckling, T.-J. Huang, and M.-H. Wu, "Ethnic differences in western and asian sacroiliac joint anatomy for surgical planning of minimally invasive sacroiliac joint fusion," *Diagnostics*, vol. 13, p. 883, 2 2023.

[69] D. Kainmueller, H. Lamecker, S. Zachow, and H.-C. Hege, "An articulated statistical shape model for accurate hip joint segmentation," pp. 6345–6351, IEEE, 9 2009.

[70] H. Lamecker, M. Seebass, H.-C. Hege, and P. Deuflhard, "A 3d statistical shape model of the pelvic bone for segmentation," p. 1341, 5 2004.

[71] F. Yokota, T. Okada, M. Takao, N. Sugano, Y. Tada, and Y. Sato, "Automated segmentation of the femur and pelvis from 3d ct data of diseased hip using hierarchical statistical shape model of joint structure," 2009.

[72] R. Hemke, C. G. Buckless, A. Tsao, B. Wang, and M. Torriani, "Deep learning for automated segmentation of pelvic muscles, fat, and bone from ct studies for body composition assessment," *Skeletal Radiology*, vol. 49, pp. 387–395, 3 2020.

[73] C. Wang, B. Connolly, P. F. de Oliveira Lopes, A. F. Frangi, and Örjan Smedby, "Pelvis segmentation using multi-pass u-net and iterative shape estimation," pp. 49–57, 2019.

[74] F. Kordon, A. Maier, B. Swartman, M. Privalov, J. S. E. Barbari, and H. Kunze, "Multi-stage platform for (semi-)automatic planning in reconstructive orthopedic surgery," *Journal of Imaging*, vol. 8, p. 108, 4 2022.

[75] B. Bier, F. Goldmann, J.-N. Zaech, J. Fotouhi, R. Hegeman, R. Grupp, M. Armand, G. Osgood, N. Navab, A. Maier, and M. Unberath, "Learning to detect anatomical landmarks of the pelvis in x-rays from arbitrary views," *International Journal of Computer Assisted Radiology and Surgery*, vol. 14, pp. 1463–1473, 9 2019.

[76] I. Bataeva, K. Shah, R. A. Vijayan, R. Han, N. M. Sheth, G. Kleinszig, S. Vogt, G. M. Osgood, J. H. Siewerdsen, and A. Uneri, "Intraoperative guidance of orthopaedic instruments using 3d correspondence of 2d object instance segmentations," p. 75, SPIE, 2 2021.

[77] A. J. Rezansoff, S. Caterine, L. Spencer, M. N. Tran, R. B. Litchfield, and A. M. Getgood, "Radiographic landmarks for surgical reconstruction of the anterolateral ligament of the knee," *Knee Surgery, Sports Traumatology, Arthroscopy*, vol. 23, pp. 3196–3201, 11 2015.

[78] Z. Isaac and M. E. Brassil, "Sacroiliac joint dysfunction," 2020.

[79] H. A. Zaidi, A. J. Montoure, and C. A. Dickman, "Surgical and clinical efficacy of sacroiliac joint fusion: a systematic review of the literature," *Journal of Neurosurgery: Spine*, vol. 23, pp. 59–66, 7 2015.

[80] S. M. Hermans, R. Droeghaag, M. G. Schotanus, H. van Santbrink, W. L. van Hemert, and I. Curfs, "Minimally invasive sacroiliac joint fusion vs conservative management in patients with sacroiliac joint dysfunction: A systematic review and meta-analysis," *International Journal of Spine Surgery*, vol. 16, pp. 472–480, 6 2022.

[81] D. W. Polly, J. Swofford, P. G. Whang, C. J. Frank, J. A. Glaser, R. P. Limoni, D. J. Cher, K. D. Wine, and J. N. Sembrano, "Two-year outcomes from a randomized controlled trial of minimally invasive sacroiliac joint fusion vs. non-surgical management for sacroiliac joint dysfunction," *International Journal of Spine Surgery*, vol. 10, p. 28, 1 2016.

[82] E. M. Randers, P. Gerdhem, J. Dahl, B. Stuge, and T. J. Kibsgård, "The effect of minimally invasive sacroiliac joint fusion compared with sham operation: study protocol of a prospective double-blinded multicenter randomized controlled trial," *Acta Orthopaedica*, pp. 1–7, 10 2021.

[83] J. Dengler, D. Kools, R. Pflugmacher, A. Gasbarrini, D. Prestamburgo, P. Gaetani, D. Cher, E. V. Eeckhoven, M. Annertz, and B. Sturesson, "Randomized trial of sacroiliac joint arthrodesis compared with conservative management for chronic low back pain attributed to the sacroiliac joint," *Journal of Bone and Joint Surgery*, vol. 101, pp. 400–411, 3 2019.

[84] B. Sturesson, D. Kools, R. Pflugmacher, A. Gasbarrini, D. Prestamburgo, and J. Dengler, "Six-month outcomes from a randomized controlled trial of minimally invasive si joint fusion with triangular titanium implants vs conservative management," *European Spine Journal*, vol. 26, pp. 708–719, 3 2017.

[85] Z. Zheng, Y. Zhang, Z. Hou, J. Hao, F. Zhai, Y. Su, and J. Pan, "The application of a computer-assisted thermoplastic membrane navigation system in screw fixation of the sacroiliac joint – a clinical study," *Injury*, vol. 43, pp. 495–499, 4 2012.

[86] R. J. Fernandes, A. Gee, N. Schneider, A. J. Kanawati, C. S. Bailey, and P. Rasoulinejad, "Accuracy of patient-specific drill guide template for bilateral c1-c2 laminar screw placement: A cadaveric study," *World Neurosurgery*, vol. 162, pp. e225–e234, 6 2022.

[87] B. Garg, M. Gupta, M. Singh, and D. Kalyanasundaram, "Outcome and safety analysis of 3d-printed patient-specific pedicle screw jigs for complex spinal deformities: a comparative study," *The Spine Journal*, vol. 19, pp. 56–64, 1 2019.

[88] N. Dea, C. G. Fisher, J. Batke, J. Strelzow, D. Mendelsohn, S. J. Paquette, B. K. Kwon, M. D. Boyd, M. F. Dvorak, and J. T. Street, "Economic evaluation comparing intraoperative cone beam ct-based navigation and conventional fluoroscopy for the placement of spinal pedicle screws: a patient-level data cost-effectiveness analysis," *The Spine Journal*, vol. 16, pp. 23–31, 1 2016.

[89] N. Kampkuiper, J. Nellensteijn, E. Heckman, S. Lankheet, M. Koenrades, and F. Schröder, "Patient-specific 3d virtual surgical planning using virtual simulated fluoroscopic images to improve sacroiliac joint fusion: a retrospective cohort study,"

[90] P. A. Pijpker, J. Kraeima, M. J. Witjes, D. M. Oterdoom, R. A. Vergeer, M. H. Coppes, R. J. Groen, and J. M. Kuijlen, "Accuracy of patient-specific 3d-printed drill guides for pedicle and lateral mass screw insertion," *Spine*, vol. 46, pp. 160–168, 2 2021.

[91] C. G. T. Ledonio, D. W. Polly, and M. F. Swiontkowski, "Minimally invasive versus open sacroiliac joint fusion: Are they similarly safe and effective?," *Clinical Orthopaedics Related Research*, vol. 472, pp. 1831–1838, 6 2014.

[92] T. Y. Wang, S. M. Bergin, K. R. Murphy, M. M. Abd-El-Barr, P. Grossi, C. I. Shaffrey, C. Crutcher, and K. D. Than, "Sacroiliac joint fusion using robotic navigation: Technical note and case series," *Operative Neurosurgery*, 4 2022.

[93] Y. R. Rampersaud, D. A. Simon, and K. T. Foley, "Accuracy requirements for image-guided spinal pedicle screw placement," *Spine*, vol. 26, pp. 352–359, 2 2001.